

General Disclaimer

One or more of the Following Statements may affect this Document

- This document has been reproduced from the best copy furnished by the organizational source. It is being released in the interest of making available as much information as possible.
- This document may contain data, which exceeds the sheet parameters. It was furnished in this condition by the organizational source and is the best copy available.
- This document may contain tone-on-tone or color graphs, charts and/or pictures, which have been reproduced in black and white.
- This document is paginated as submitted by the original source.
- Portions of this document are not fully legible due to the historical nature of some of the material. However, it is the best reproduction available from the original submission.

(NASA-CR-170721) STUDY OF TETHERED
SATELLITE ACTIVE ATTITUDE CONTROL Interim
Report, 1 Mar. - 31 Aug. 1982 (Smithsonian
Astrophysical Observatory) 71 p
HC A04/MF A01

N83-17570

Unclas
02740

CSCI 22B G3/15

STUDY OF
TETHERED SATELLITE
ACTIVE ATTITUDE CONTROL

CONTINUATION OF
INVESTIGATION OF ELECTRODYNAMIC STABILIZATION AND
CONTROL OF LONG ORBITING TETHERS

Contract NAS8-33691

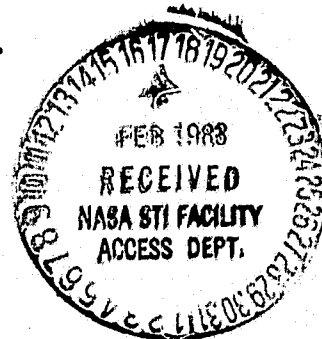
Interim Report

For the period 1 March 1982 through 31 August 1982

Principal Investigator

Dr. Giuseppe Colombo

October 1982



Smithsonian Institution
Astrophysical Observatory
Cambridge, Massachusetts 02138

The Smithsonian Astrophysical Observatory
and the Harvard College Observatory
are members of the
Center for Astrophysics

STUDY OF
TETHERED SATELLITE
ACTIVE ATTITUDE CONTROL

CONTINUATION OF
INVESTIGATION OF ELECTRODYNAMIC STABILIZATION AND
CONTROL OF LONG ORBITING TETHERS

Interim Report

For the period 1 March 1982 through 31 August 1982

Principal Investigator

Dr. Giuseppe Colombo

Co-Investigator

Mr. David Arnold

List of Figures

	<u>Page</u>
Figure 2-1. Reference Frame for Motion of Subsatellite About Tether Attach Point.	4.
Figure 2-2. Reference Frame for Motion of Subsatellite About It's Center of Mass (G).	6.
Figure 2-3. Graphical Solution for Stationary Conditions (Equations 17 and 19).	11.
Figure 2-4. Two Stationary Relative Configurations seen in the Direction of the Orbital Velocity Vector	13.
Figure 3-1. Geometry of the Rotational Test Case.	21.
Figure 3-2. Spinning Subsatellite Stable Configuration. Software Test Case (a) DUMBEL: θ vs. Time.	23.
Figure 3-2. (b) DUMBEL: ψ' vs. Time (ψ' is in Rotating Co-ordinate System).	24.
Figure 3-2. (c) DUMBEL: ϕ vs. Time	25.
Figure 3-3. Spinning Subsatellite Stable Configuration. Software Test Case (a) SKYHOOK: θ vs. Time	32.
Figure 3-3. (b) SKYHOOK: ψ vs. Time (ψ is in Inertial Co-Ordinate System which Results in Linear Increase of ψ with Time).	33.
Figure 3-3. (c) SKYHOOK: ϕ vs. Time.	34.
Figure 3-4. Attitude Thruster Test Case (a) Inclination Angle (θ) vs. Time	36.
Figure 3-4. (b) Nodal Angle ψ vs. Time.	37.
Figure 3-4. (c) Spin Angle ϕ vs. Time	38.
Figure 3-5. Subsatellite Torque Vector Conventions.	40.

Table of Contents

	<u>Page</u>
1.0 Introduction.	1.
2.0 A Simplified Model of the Motion About the Center of Mass of a Tethered Subsatellite.	2.
2.1 Introduction.	2.
2.2 The Simplified Model.	2.
2.3 Notation and Reference Frame.	3.
2.4 Dynamical Equations	7.
2.5 Stationary Solution	8.
2.6 Stability of the Equilibrium Configurations	12.
2.7 Conclusions	17.
3.0 Rotational Dynamics Software Development and Verification . . .	18
3.1 Two-Mass Tether Model (DUMBEL).	18.
3.1.1 Adaptation of DUMBELL Rotational Dynamics Model to the VAX.	18.
3.1.2 Verification of Two Mass Tether Models Using Rotational Test Case	19.
3.2 Multiple-Mass Tether Model (SKYHOOK).	25.
3.2.1 SKYHOOK Tether Model with Subsatellite Rotational Dynamics Capability.	26.
3.2.2 Testing of SKYHOOK with Rotational Dynamics.	30.
3.3 Behavior of a Subsatellite with a Single Thruster	31.
4.0 Adaptation of SKYHOOK General Rotational Dynamics Model to Specific Attitude Control Systems.	39.
APPENDIX.	A-1.
Rotational Dynamics of Subsatellite Vehicle	

1.0 Introduction

This Interim Report summarizes the work performed under Modification 7 of Contract NAS8-33691 entitled "Study of Tethered Satellite Active Attitude Control." Under this modification, SAO adapted existing software for the study of tethered subsatellite rotational dynamics to its present data processing system, developed an analytic solution for a stable configuration of a tethered subsatellite, compared the analytic and numerical integrator (computer) solutions for this "test case" in a two-mass tether model program (DUMBEL), modified the existing SAO multiple-mass tether model (SKYHOOK) to include subsatellite rotational dynamics, verified this modification with the analytic "test case," and demonstrated the use of the SKYHOOK rotational dynamics capability with a computer run showing the effect of a single off-axis thruster on the behavior of the subsatellite.

SAO is now in a position to develop subroutines for specific attitude control systems and to apply them to the study of the behavior of the tethered subsatellite under realistic on-orbit conditions. Such studies could also include the effect of all tether "inputs," including pendular oscillations, air drag, and electrodynamic interactions, on the dynamic behavior of the tether.

2.0 A Simplified Model of the Motion About the Center of Mass of a Tethered Subsatellite

2.1 Introduction

The dynamics of a tethered subsatellite about its center of mass is quite complex in the general case and required sophisticated changes to the SKYHOOK program. SKYHOOK has been rewritten to deal with any tethered subsatellite mission requiring high accuracy attitude prediction and control such as astronomical or earth observation missions or, more generally, any mission which depends heavily on isolation of the package from the noise coming from the connection to the Shuttle through the tether. For acquiring experience and physical insight into the dynamics of this system and for providing an analytical solution against which the program changes could be checked, we have studied a simple configuration which can be solved analytically.

2.2 The Simplified Model

We consider the shuttle in a circular orbit (nominal low orbit at 150 n.m. = 270 km altitude here, but this is not a very critical constraint) and assume that the orbit is polar or equatorial. The orbital plane is therefore invariable in an inertial frame.

We also assume that the subsatellite is axially symmetric with the point of attachment of the tether (O) being a point on the symmetric axis of the subsatellite different from G, the center-of-gravity of the subsatellite. We also call C the moment of inertia of the subsatellite with respect to the symmetry axis and A, the moment of inertia with respect to an equatorial axis. In this model we neglect the dynamics of the tether induced by the rotational motion of the subsatellite and we assume also that there is no significant in-plane or out-of-plane oscillation of the tether and subsatellite.

ORIGINAL PAGE IS
OF POOR QUALITY

We neglect also the longitudinal oscillation of the tether-subsatellite system. The motion of the subsatellite is therefore equivalent to the motion of a axis-symmetric rigid-body about its center of mass when a force constant in magnitude and rotating uniformly about an axis normal to the force and constant in orientation (in this case normal to the orbital plane) is applied to a point, P, of its symmetry axis. Other torques and the effects of the precession of the orbital plane may be introduced into the computer model but are difficult to deal with analytically.

2.3 Notation and Reference Frame

In Figure 2-1 E is the center of Earth; S, the Shuttle considered as a point; O, the attachment point of the subsatellite; \underline{a} , the unit vector from E to S to O; \underline{c} , the unit vector normal to the orbital plane; $\underline{b} = \underline{c} \times \underline{a}$, the unit vector tangent to the orbit; G the center-of-mass of the subsatellite; d, the distance from O to G; \underline{k} , a unit vector in the direction from O to G; \underline{i} and \underline{j} , two orthogonal unit vectors in the plane normal to the symmetry axis O-G which equals $\underline{k}d$; \underline{N} , the nodal line intersection of the plane O, \underline{i} , \underline{j} with the orbital plane; ψ , ϕ , θ , the Eulerian angles of the frame O, \underline{i} , \underline{j} , \underline{k} , with respect to the frame O, \underline{a} , \underline{b} , \underline{c} and \underline{F} , the gravity gradient force acting on G which is equal to the tension in the tether. We neglect the gravity gradient torque acting on the body which is negligible if the dimensions of the body are small with respect to the length of the tether (ℓ) and which is true for virtually all subsatellites. In good approximation we may write:

$$\underline{F} = 3g(\gamma)M\left(\frac{\ell}{a}\right) \left[1 + \sigma\left(\frac{d}{\ell}\right) + \sigma \left| \frac{(C-A)n^2 a}{Md \ell g(\ell)} \right| \right] \quad (1)$$

ORIGINAL PAGE IS
OF POOR QUALITY

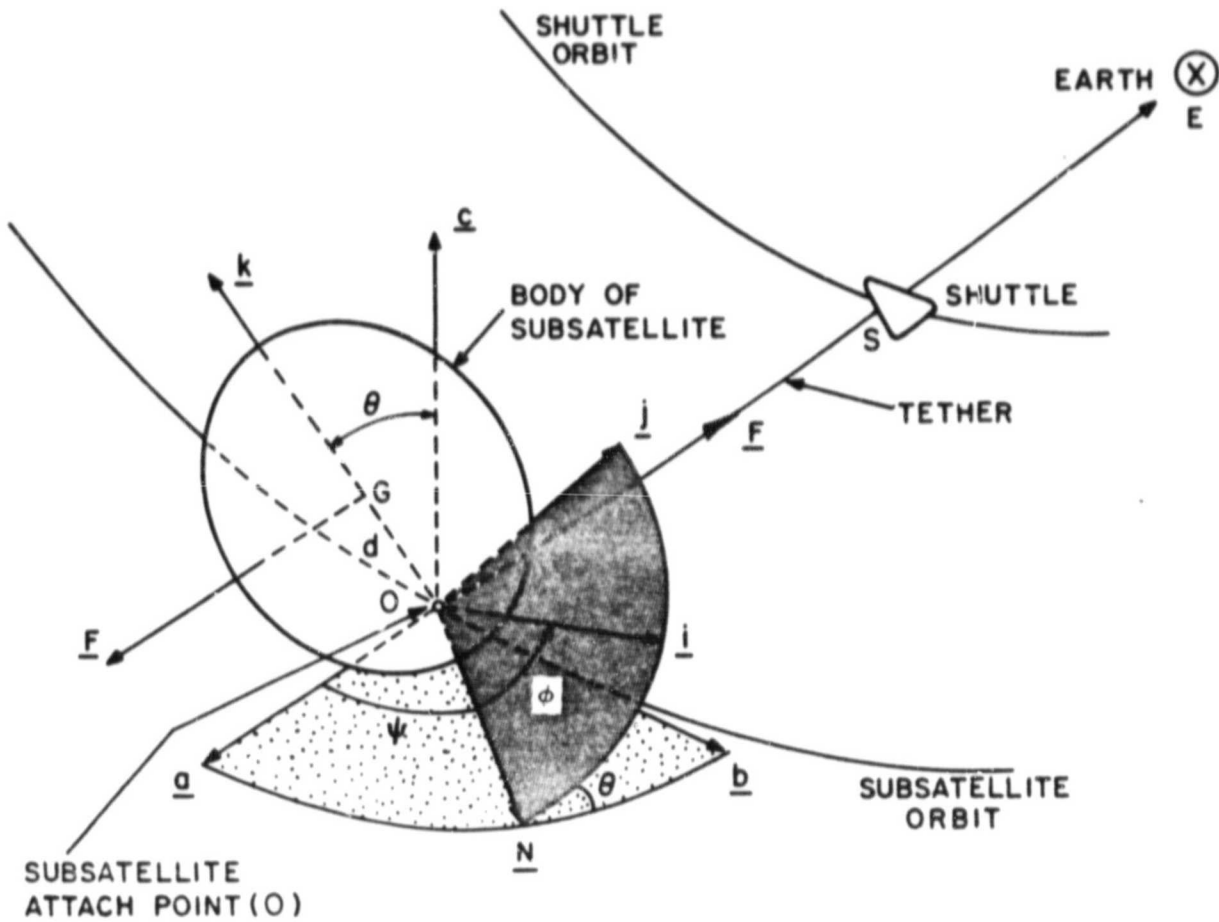


Figure 2-1. Reference Frame for Motion of Subsattellite About Tether Attach Point .

Here $g(0)$ is the acceleration of gravity at 0, M is the mass of the subsatellite; n , the orbital mean motion, $\sigma(x)$ is a coefficient of magnitude x with respect to λ , and where the quantities denoted by σ are infinitesimally small. As an example, if $d = 0.5m$, $\lambda = 50$ km, $C-A = M(0.5m)^2$, $n = 10^{-3}$, $g(0) = 9$ m/sec², we have

$$\sigma\left(\frac{d}{\lambda}\right) = 10^{-5} \quad (2-1)$$

and

$$\sigma\left[\frac{(C-A)n^2 a}{M d \lambda g(0)}\right] = \frac{0.25 \times 10^{-6} \times 6.7 \times 10^6}{0.5 \cdot 5 \times 10^4 \cdot 9} = 10^{-5} \quad (2-2)$$

This evaluation gives an idea of the magnitude of the terms which are neglected. If λ is of the order of 1 km and d is of the order of 1 cm, $\sigma\left(\frac{d}{\lambda}\right)$ is of magnitude, 10^{-5} , while the second term is on the order of 2.5×10^{-2} . Only if d is down to the mm level and λ is down to the 0.1 km level, is the second term on the same order as the main term.

A second reference system (see Figure 2-2) is obtained by displacing the center of the frame to the point G. This is done when we want to consider the motion of the subsatellite, in the classical way, about its center of mass. The only torque affecting this motion in the system being analyzed here is the torque T due to the tension applied by the tether to the subsatellite. Its value is

$$\underline{T} = (-d\underline{k}) \times (-3g(0)\frac{M\lambda}{a}\underline{a}) = 3g(0)\frac{M\lambda d}{a}\underline{k} \times \underline{a} \quad (3)$$

Before passing to the equations of motion we define the Eulerian angle since different notations are used here than in the literature.

The angle ψ is the angle measured in the plane \underline{a} , \underline{b} , from \underline{a} to \underline{N} (nodal line) counterclockwise (c.c.w.) with respect to an observer standing along \underline{c} ; θ is the angle from \underline{c} to \underline{k} measured c.c.w. from an observer oriented along \underline{N} ; ϕ is the angle between \underline{N} and \underline{i} measured c.c.w. from an observer oriented as \underline{k} .

ORIGINAL PAGE IS
OF POOR QUALITY

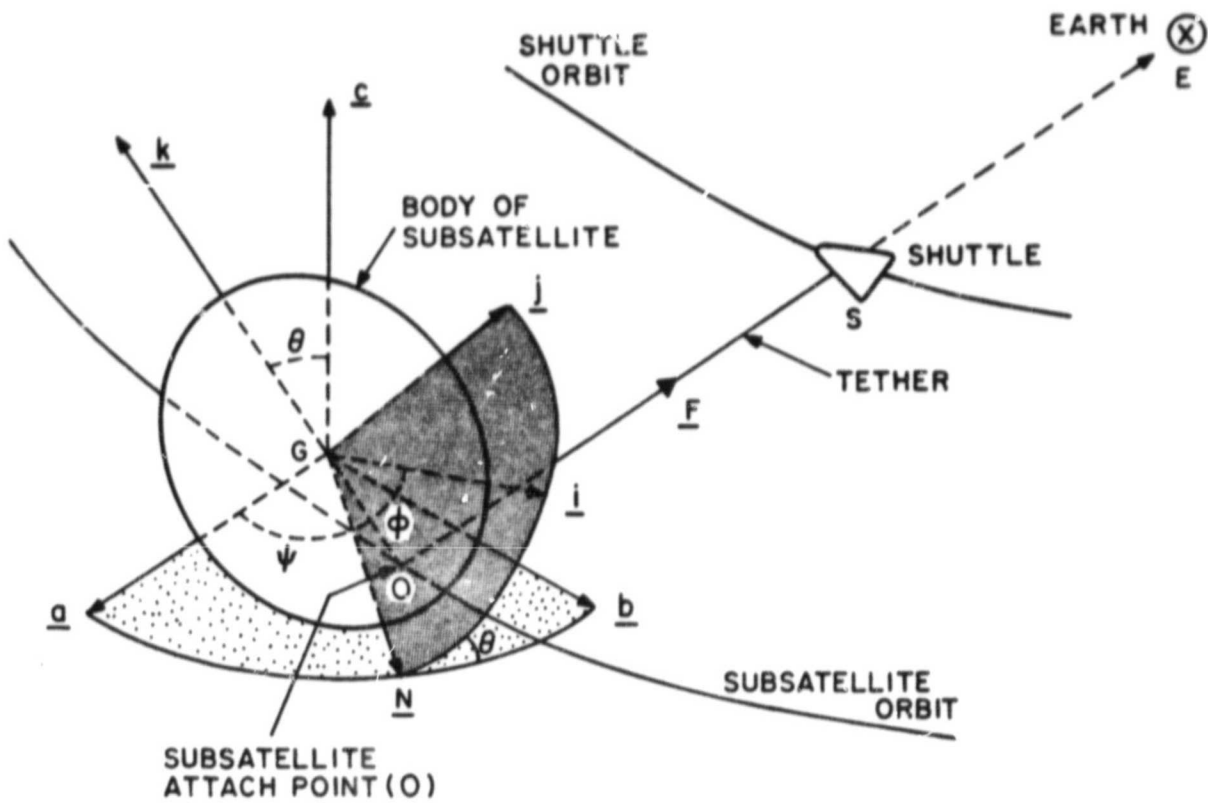


Figure 2-2. Reference Frame for Motion of Subsattellite about It's Center of Mass (G).

Concerning the torque given by (3), notice that we neglect the feedback effect of the tether mass on the motion that we are analyzing. We also neglect the possible variation of the orientation of the tether from the vertical direction. The general computer model includes both these effects.

2.4 Dynamical Equations

The following is the standard procedure for writing the expression of kinetic energy with respect to an absolute frame

$$T = \frac{1}{2} \left\{ A [\dot{\theta}^2 + (\dot{\psi} + n)^2 \sin^2 \theta] + C [\dot{\phi} + (\dot{\psi} + n) \cos \theta]^2 \right\} \quad (4)$$

The work done by the force \underline{F} is given by (see Figure 2-1)

$$\begin{aligned} -\underline{F} \cdot \underline{\delta O} &= -|\underline{F}| \underline{a} \cdot \delta(-d\underline{k}) = |\underline{F}| d\underline{a} \cdot \delta\underline{k} \\ &= |\underline{F}| d \delta(\sin \theta \sin \psi) \\ &= |\underline{F}| d (\delta \theta \cos \theta \sin \psi + \delta \psi \sin \theta \cos \psi) \end{aligned} \quad (5)$$

where δ denotes a small variation in the quantity. The modules of the vector \underline{F} are denoted by F , below.

The Lagrangian equations become:

$$\frac{d}{dt} (A\dot{\theta}) - A(\dot{\psi} + n)^2 \sin \theta \cos \theta + C[\dot{\phi} + (\dot{\psi} + n) \cos \theta] (\dot{\psi} + n) \sin \theta = F d \cos \theta \sin \psi \quad (6-1)$$

$$\frac{d}{dt} \left[A(\dot{\psi} + n) \sin^2 \theta + C[\dot{\phi} + (\dot{\psi} + n) \cos \theta] \cos \theta \right] = F d \sin \theta \cos \psi \quad (6-2)$$

$$\frac{d}{dt} \left[C[\dot{\phi} + (\dot{\psi} + n) \cos \theta] \right] = 0 \quad (6-3)$$

From the last equation we have

$$\dot{\phi} + (\dot{\psi} + n) \cos \theta = r_0 \quad (7)$$

This relation means that the component of the angular momentum along the symmetry axis and of the angular velocity with respect to an absolute frame is constant. The equations (6-1) and (6-2) become:

$$A\ddot{\theta} - A(\dot{\psi}+n)^2 \sin\theta \cos\theta + Cr_0(\dot{\psi}+n)\sin\theta = Fd\cos\theta \sin\psi \quad (8-1)$$

$$A\ddot{\psi} \sin\theta + 2A\dot{\theta}(\dot{\psi}+n)\cos\theta - Cr_0\dot{\theta} = Fd\cos\psi \quad (8-2)$$

Equations (7) and (8) give the general solution. It should be noticed, however, that equation (8-2) becomes singular for $\theta = 0$, and therefore, the numerical integration may "blow-up" at this point.

2.5 Stationary Solution

One may search for stationary solutions. For instance, one may search for solutions that satisfy the relation

$$\theta = \theta_0 \neq 0 \quad (9)$$

Equations (8-1) and (8-2) become

$$-A(\dot{\psi}+n)^2 \sin\theta_0 \cos\theta_0 + Cr_0(\dot{\psi}+n)\sin\theta_0 - Fd\cos\theta_0 \sin\psi = 0 \quad (10-1)$$

$$A\ddot{\psi} \sin\theta_0 - Fd\cos\psi = 0 \quad (10-2)$$

Multiplying (10-2) by $\dot{\psi}$ one yields

$$\frac{1}{2} A\dot{\psi}^2 \sin\theta_0 - Fd\sin\psi = H_0 \quad (11)$$

while equation (10-1) may be written

$$-A\dot{\psi}^2 - 2A\dot{\psi}n\sin\theta_0 \cos\theta_0 - An^2 \sin\theta_0 \cos\theta_0 + Cr_0(\dot{\psi}+n)\sin\theta_0 - Fd\cos\theta_0 \sin\psi = 0 \quad (12)$$

or

$$A\dot{\psi}^2 + Fd\cos\theta_0 \sin\psi - An^2 \sin\theta_0 \cos\theta_0 = 0 \quad (13)$$

and

$$2An\sin\theta_0 \cos\theta_0 - Cr_0 \sin\theta_0 = 0 \quad (14)$$

For (11) to be identical to (13), one should have

$$\frac{2}{\sin\theta_0} = \cos\theta_0, \sin\theta_0 \cos\theta_0 = 2 \quad (15)$$

which does not have any solution. The only solution $\theta = \theta_0$ are obtained with $\psi = \psi_0 = \pm \frac{\pi}{2}$ and

$$-An^2 \sin\theta_0 \cos\theta_0 + C\phi_0 n \sin\theta_0 \pm Fd \cos\theta_0 = 0 \quad (16)$$

where the signs (-) and (+) hold, respectively, when $\psi = \pm \frac{\pi}{2}$.

One should notice that any solution $\psi = \frac{\pi}{2}$, $\theta = \theta_0$ is coincident with the solution $\psi = -\frac{\pi}{2}$, $\theta = -\theta_0$. Therefore, we shall consider only the case $\psi = \frac{\pi}{2}$. Equation (16), where we hold the sign (-) in front of the term $Fd \cos\theta_0$ ($\psi = \frac{\pi}{2}$), and taking into account (7) yields

$$(C-A)n^2 \sin\theta_0 \cos\theta_0 + C\dot{\phi}_0 n \sin\theta_0 - Fd \cos\theta_0 = 0 \quad (17)$$

If $\dot{\phi}_0 \gg n$ equation (17) reduces to

$$\tan\theta_0 = \frac{Fd}{C\dot{\phi}_0 n} \quad (18)$$

If $C\dot{\phi}_0$ and $(C-A)n$ are comparable, we can solve equation (17). We may write equation (17) in the form

$$\frac{C-A}{2} n^2 \sin 2\theta_0 = -Q \sin(\theta_0 - \beta_0) \quad (19)$$

where

$$Q = |(C^2 \dot{\phi}_0^2 n^2 + F^2 d^2)^{1/2}| \quad (20-1)$$

$$\sin\beta_0 = Fd/Q, \cos\beta_0 = C\dot{\phi}_0 n/Q \quad (20-2)$$

Solution of equation (19) is given graphically in Figure 2-3. The corresponding configurations are illustrated in Figure 2-4. It is clear that when $(C-A)\frac{n^2}{2} \ll Q$ solution of (19) gives $\theta_0 = \beta_0$ and $\theta_0 = \beta_0 + (2n+1)\pi$.

As an example we take:

$$\begin{aligned}d &= 0.1 \text{ m}, C = M(0.5\text{m})^2, A = M(0.3\text{m})^2, \\ \lambda &= 10 \text{ km}, g(0) = 9\text{m/sec}^2, n = 10^{-3}, \\ F &= 3 \times 9 \times M \times \frac{10}{6700} = \frac{2.7}{67} M, \\ \dot{\phi}_0 &= 10^{-1}.\end{aligned}$$

Then equation (17) becomes

$$\begin{aligned}0.16M \times 10^{-6} \sin\theta_0 \cos\theta_0 + 0.25M \times 10^{-4} \sin\theta_0 \\ - \frac{2.7M \times 0.1 \cos\theta_0}{67} = 0\end{aligned}\tag{21}$$

which gives, in first approximation

$$\begin{aligned}\tan\theta_0 &= 10^{11}, \theta_0 = 89^\circ 43' \\ \theta_0 &= 269^\circ 43'\end{aligned}\tag{22}$$

If $\dot{\phi}_0 = 10^{-2}$ we will have

$$\begin{aligned}\tan\theta_0 &= 10, \theta_0 = 84^\circ 29' \\ \theta_0 &= 264^\circ 29'\end{aligned}\tag{23}$$

Now introduce the small angle

$$\Delta\theta = \theta_0 - \beta_0\tag{24}$$

where θ_0 is the solution of (19), we have

$$\frac{C-A}{2} n^2 (\sin 2\beta_0 + 2\Delta\theta \cos 2\beta_0) = -Q\Delta\theta\tag{25}$$

ORIGINAL PAGE IS
OF POOR QUALITY

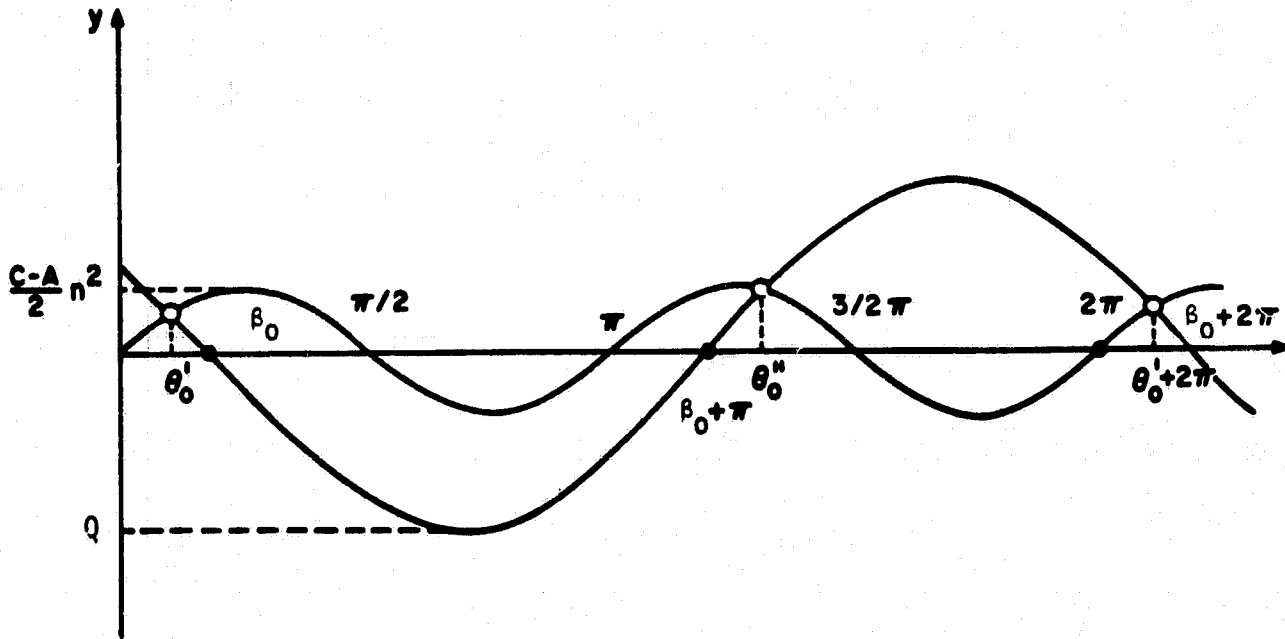


Figure 2-3. Graphical Solution for Stationary Conditions (Equations 17 and 19).

and, therefore

$$\Delta\theta = -\frac{(C-A)n^2\sin 2\theta_0}{2Q + 2(C-A)n^2 \cdot \cos 2\theta_0} \quad (26)$$

From which we may evaluate the first order correction.

Considering only the case $\dot{\phi}_0 = 10^{-2}$, we have for the two steady state configurations

$$\Delta\theta_1 = -\frac{0.16 \times 0.034}{2 \times 2.51 \times 10^3} \text{ rad} = 0.22 \text{ arc seconds} \quad (27.1)$$

$$\Delta\theta_2 = -\frac{0.16 \times 0.19}{2 \times 2.51 \times 10^3} \text{ rad} = 1.25 \text{ arc seconds} \quad (27.2)$$

We conclude by noticing that even if $\dot{\phi}_0 = 0.1n$, or one tenth of the mean motion, the correction is negligible.

2.6 Stability of the Equilibrium Configurations

Since there are only two configurations of equilibrium, one presumes that one will be stable while the other is unstable. This may be the case, but, since we are confronted with the complex behavior of a three degree of freedom system here, other steady state solutions may exist and one must be careful in reaching general conclusions from this analysis in order to evaluate the stability of these configurations. The equations (8) are time independent as the Lagrangian function from which they are deduced which is:

$$L = T + U = 1/2 \left\{ A[\dot{\theta}^2 + (\dot{\psi}+n)^2\sin^2\theta] + C[\dot{\phi} + (\dot{\psi}+n)\cos\theta]^2 \right\} - F\sin\theta\sin\psi \quad (28)$$

The system has a first integral (7) which implies the invariability with respect to time of the component of the angular velocity vector along the symmetry axis, and the corresponding component of the angular momentum

$$Cr_0 = C[\dot{\phi} + (\dot{\psi}+n)\cos\theta] \quad (29)$$

ORIGINAL PAGE IS
OF POOR QUALITY

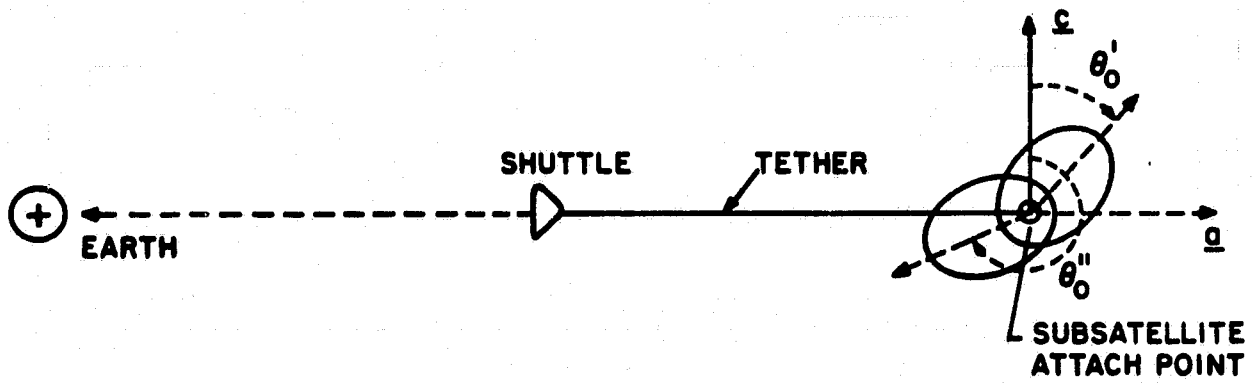


Figure 2-4. Two Stationary Relative Configurations seen in the Direction of the Orbital Velocity Vector.

Moreover, the energy integral holds

$$1/2 \left\{ A \dot{\theta}^2 + (\dot{\psi} + n)^2 \sin^2 \theta + Cr_0^2 \right\} - F \sin \theta \sin \psi = E \quad (30)$$

Next we consider the linear stability of the steady state solution defined by the following initial conditions:

$$\begin{aligned} \theta(0) &= \theta_0, \quad \dot{\theta}(0) = 0, \quad \psi(0) = \frac{\pi}{2}, \quad \dot{\psi}(0) = 0, \\ \dot{\phi} &= \dot{\phi}_0 = r_0 - n \cos \theta_0 \end{aligned} \quad (31)$$

where θ_0 is one of the two solutions of equation (16) or (17), while ϕ , being a cyclic variable, may be chosen arbitrarily.

We consider the equations (7) and (8) and make the following assumptions:

$$\begin{aligned} \theta &= \theta_0 + \epsilon \theta_1, \quad \psi = \frac{\pi}{2} + \epsilon \psi_1, \quad \dot{\psi} = \epsilon \dot{\psi}_1 \\ \dot{\phi} &= \dot{\phi}_0 + \epsilon \dot{\phi}_1, \quad r = r_0 + \epsilon r_1 \end{aligned} \quad (32)$$

and substitute these in equations (7), (8), considering ϵ a first order quantity. Neglecting second order quantities in ϵ we have from (7)

$$r_0 + \epsilon r_1 = \dot{\phi}_0 + \epsilon \dot{\phi}_1 + (\epsilon \dot{\psi}_1 + n) \cos(\theta_0 + \epsilon \theta_1) \quad (33)$$

From which we get

$$r_1 = \dot{\phi}_1 + \dot{\psi}_1 \cos \theta_0 - n \theta_1 \sin \theta_0 \quad (34)$$

Since, however, the first integral holds also for the new initial conditions, we have

$$\dot{\phi}_1 + \dot{\psi}_1 \cos \theta_0 - n \theta_1 \sin \theta_0 = (r_1)_0 \quad (35)$$

which implies that if θ_1, ψ_1 , remain small in the perturbed motion then ϕ_1 , will also remain small. Therefore, we have to study the stability with respect to the two variables θ and ψ because the stability of ϕ is

derived from (35). As a matter of fact, we consider only the subset of motions which correspond to the same value of r_0 that in turn defines through equation (16) the value of θ_0 , and ignore the ϕ coordinate. For other values of r_0 different equilibrium configurations occur. For each of them the same assumptions and the deductions obtained here hold.

Consider equations (8) and substitute (32) keeping r_0 constant. We arrive at the following equations:

$$\begin{aligned}
 \epsilon A \ddot{\theta}_1 - \frac{A}{2} (\epsilon \dot{\psi}_1 + n)^2 \sin 2(\theta_0 + \epsilon \theta_1) + Cr_0 (\epsilon \dot{\psi}_1 + n) \sin (\theta_0 + \epsilon \theta_1) \\
 = Fd \cos (\theta_0 + \epsilon \theta_1) \sin \left(\frac{\pi}{2} + \epsilon \psi_1 \right) \\
 \epsilon A \ddot{\psi}_1 \sin (\theta_0 + \epsilon \theta_1) + 2A \epsilon \dot{\theta}_1 (\epsilon \dot{\psi}_1 + n) \cos (\theta_0 + \epsilon \theta_1) - Cr_0 \epsilon \dot{\theta}_1 \\
 = Fd \cos \left(\frac{\pi}{2} + \epsilon \psi_1 \right)
 \end{aligned} \tag{36}$$

Neglecting second order quantities and taking into account that θ_0 is a solution of equation (16) we write the following linear system with constant coefficients

$$\begin{aligned}
 A \ddot{\theta}_1 - (2An \sin \theta_0 \cos \theta_0 - Cr_0 \sin \theta_0) \dot{\psi}_1 \\
 + [Cr_0 n \cos \theta_0 + Fd \sin \theta_0 - An^2 \cos 2\theta_0] \theta_1 = 0 \\
 A \ddot{\psi}_1 \sin \theta_0 + (2An \cos \theta_0 - Cr_0) \dot{\theta}_1 + Fd \psi_1 = 0
 \end{aligned} \tag{37}$$

The linear system (37) has the following characteristic equations

$$\begin{aligned}
 (\lambda^2 A \sin \theta_0 + Fd)(\lambda^2 A + Cr_0 n \cos \theta_0 + Fd \sin \theta_0 - An^2 \cos 2\theta_0) \\
 + (2An \cos \theta_0 - Cr_0)^2 \sin \theta_0 \lambda^2
 \end{aligned} \tag{38}$$

that is, the quadratic equation

ORIGINAL PAGE IS
OF POOR QUALITY

$$\begin{aligned} & \mu^2 A^2 \sin^2 \theta_0 + \mu \left\{ AFd(1+\sin^2 \theta_0) - 3ACr_0 \cos \theta_0 \sin \theta_0 \right. \\ & + 3A^2 [n^2 \cos^2 \theta_0 \sin \theta_0 + A^2 n^2 \sin^3 \theta_0] + C^2 r_0^2 \sin \theta_0 \left. \right\} \\ & + dF (Cr_0 n \cos \theta_0 + Fd \sin \theta_0 - An^2 \cos 2\theta_0 \end{aligned} \quad (39)$$

where we substitute μ for λ^2 . Since the system is a Lagrangian conservative system the characteristic exponents which are solutions of equation (39) either are real or imaginary; they cannot be complex. Therefore equation (39) certainly has real solutions μ_1 and μ_2 . Stability occurs when both solutions are negative which means that the three coefficients of equation (40) should have the same sign.

A general discussion of the signs of the coefficients are very complex. Some limiting cases may be treated easily. In particular, let us consider equation (16) choosing the negative sign in front of the last term, which we will rewrite here,

$$An^2 \sin \theta_0 \cos \theta_0 - Cr_0 n \sin \theta_0 + Fd \cos \theta_0 = 0 \quad (40)$$

and assume that

$$An^2 \ll Cr_0 n, \quad An^2 \ll Fd \quad (41)$$

From (40) we have

$$Cr_0 n \sin \theta_0 - Fd \cos \theta_0 = 0 \quad (42)$$

Similarly, equation (39) becomes

$$\begin{aligned} & \mu^2 A^2 n^2 \sin^2 \theta_0 + \mu \sin \theta_0 \left\{ F^2 d^2 \cos^2 \theta_0 + An^2 Fd (1 + \sin^2 \theta_0 - 3 \cos^2 \theta_0) \right\} \\ & + F^2 d^2 n^2 = 0 \end{aligned} \quad (43)$$

From (43) we see that for $\theta_0 = \theta_0'$ the three coefficients are all positive and the solution is stable, while for $\theta_0 = \theta_0''$, the second coefficient is negative and the configuration is unstable. In the same way we may analyze the limiting case $Fd \ll An^2$, $Fd \ll Cr_0 n$, and the case $Cr_0 n \ll Fd$, and $Cr_0 n \ll An^2$.

2.7 Conclusions

We have in this part of the report considered a very simple dynamic model which provides a tool for checking the numerical integration program. For any more complex model analytical treatment will require a larger effort particularly if we want to take into account possible eccentricities of the orbit, and the regression of the node (that is, the motion of the orbital plane). We could have easily found some steady state configuration for a triaxial body but we thought we would not have learned much more by doing so. However, we do believe that an extension of this analytical study to a more sophisticated model would be necessary for a full understanding of the system. In fact, while the numerical integration of the general system as described in this report could be quite expensive in the general case we think that the numerical integration of equation (6) or of the corresponding equations for a more realistic model (which may take into account the triaxiality of the body, the orbital eccentricity, and the regression of the orbital plane) will be much less demanding in term of computing time and will lead to a better understanding of the dynamics of the system.

3.0 Rotational Dynamics Software Development and Verification

3.1 Two-Mass Tether Model (DUMBEL)

3.1.1 Adaptation of DUMBELL Rotational Dynamics Model to the VAX

Annex III of the Final Report for NASA Contract NAS8-32199, "Study of the Dynamics of a Tethered Satellite System (SKYHOOK)," March 1978 (attached as an Appendix to this report) describes a version of the DUMBEL computer program which models the rotation of the subsatellite. The program integrates the motion of two masses - the Shuttle which is considered to be a point mass and the subsatellite which is modelled as a rigid-body with three moments of inertia and an attachment point to the tether. The rotation is described by twelve variables using the method of direction cosines (nine quantities) together with the three angular velocities about the principle axes. Six variables give the state vector of the center of mass of the subsatellite and another six give the state vector of the Shuttle for a total of twenty-four variables. The tether is assumed to be a massless visco-elastic connection whose dynamics is not represented by any mass points or integration variables.

The rotational dynamics version of the DUMBEL program was written on a CDC 6400 computer and has not been used since the original study under which it was developed. In preparation for the current study of subsatellite rotation, this program was converted to the VAX computer currently in use at SAO. Changes have been made to allow the program to be run in an interactive mode with the necessary input parameters being supplied through an interactive terminal. (Batch mode operation can also be done using a prepared file of input parameters.)

In order to verify successful conversion of this program to the VAX, an original CDC 6400 run was duplicated on the VAX with initial conditions of

$\psi = 20^\circ$, $\theta = 0^\circ$, and $\phi = 0^\circ$. All initial angular velocities were zero. The initial angles are converted to direction cosines for the integration of the dynamics and then the direction cosines are converted back to Euler angles at each output point. At the beginning of the integration, the output angles should be the same as the input angles. After debugging, inspection of the original and new printouts showed only small differences between the output angles which are assumed to be due to the better numerical precision on the VAX computer in double precision.

3.1.2 Verification of Two Mass Tether Models Using Rotational Test Case

The test case (solved analytically in 2.0, above) consists of a special stationary solution of the equations of motion in which the axis of rotation of a symmetrical subsatellite maintains a fixed orientation with respect to the tether. This is accomplished by having the precession rate of the subsatellite equal to the orbital angular velocity. The analytic solution was obtained in a reference coordinate system rotating with the orbit and used Euler angles to describe the orientation of the subsatellite. The axis of rotation is contained in the plane defined by the direction of the tether and the normal of the plane of the orbit. The angle between the rotation axis and the normal to the orbit plane is fixed and may be either plus or minus. Assuming the Shuttle is above the subsatellite we can define positive angles as measured from the normal to the orbit toward the Shuttle, and negative angles as measured toward the earth. As the angular velocity about the symmetry axis increases the angle between the rotation axis and the normal to the orbit decreases. For high rotation speeds, the rotation axis is nearly perpendicular to the wire (and parallel to the normal to the orbit) in this special stationary solution. For zero rotation rate the angle to the orbit normal is either plus or minus 90 degrees. That is, the subsatellite is hanging either straight down or straight up. The up configura-

ORIGINAL PAGE IS
OF POOR QUALITY

tion is obviously unstable. With the proper initial conditions in this case, the subsatellite precesses at the same rate as the orbital angular velocity so that the subsatellite maintains a fixed orientation with respect to the tether. The equation giving the relation between the subsatellite angle θ and the spin angular velocity r is

$$-A n^2 \sin\theta \cos\theta + C n r \sin\theta = F d \cos\theta$$

where A is the moment of inertia in the plane of symmetry of the subsatellite, C is its moment of inertia about the symmetry axis ($C > A$), n is the orbital angular velocity, θ is the angle between the symmetry axis and the normal to the orbit plane, F is the wire tension, and d is the distance from the center of gravity to the attachment point of the tether. For a given angle θ we can solve for the required spin angular velocity r to obtain

$$r = \frac{\cos\theta}{C} \left(\frac{F d}{n \sin\theta} + A n \right)$$

The geometry must be such that the precession is in the right direction to make the symmetry axis follow the orbital motion. The proper geometry can be set up using the equation

$$\vec{N} = \vec{\tau} = \vec{d} \times \vec{F}$$

where \vec{N} is the rate of change of angular momentum, $\vec{\tau}$ is the torque, \vec{d} is vector to the attachment point, and \vec{F} is the force due to the wire tension.

The direction of spin of the subsatellite is shown on the circle around the vector d (Figure 3-1). The spin angular velocity is parallel to d and the torque is in the $-y$ direction. Since the Shuttle motion is in the $+y$ direction, the precession is in the proper direction.

The parameters used in the test run are Shuttle altitude 220 km, Shuttle mass 86.363 metric tons, subsatellite mass 100 kg, tether length 20 km,

ORIGINAL PAGE 13
OF POOR QUALITY

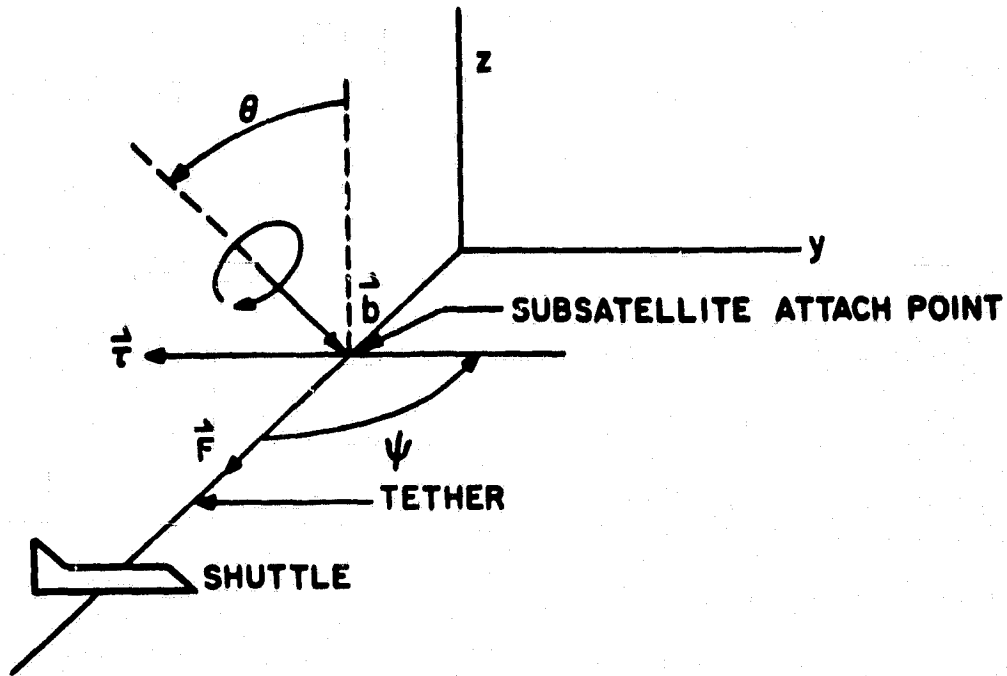


Figure 3-1. Geometry of the Rotational Test Case.

$\theta_0 = 20^\circ$, $\phi_0 = 0^\circ$, $\psi_0 = 90^\circ$, orbital angular velocity $n = 1.178021398 \times 10^{-3}$ radians/sec, $d = 50$ cm, tension force $F = .8342029979 \times 10^6$ dynes, principal moment of inertia $C = 2 \times 10^{12}$, and $A = 1 \times 10^{12}$ in c.g.s. units. The moments of inertia have been arbitrarily chosen very large in order to obtain a small value of r . A fast spin rate would result in very slow numerical integration. For the values of the parameters, the spin rate is $r = -.04919339283$ radians/sec. The initial rates of the Euler angles are $\dot{\psi}_0 = n$, $\dot{\phi}_0 = r$, and $\dot{\theta}_0 = 0$. The integration was run for 300 seconds with output points every 10 seconds. The angle θ was .3490658 radians at the beginning and increased to about .3490669 radians at the end. The value of ψ was initially 1.5707963 radians and increased to 1.9242006 radians at 300 seconds. Adding nt to ψ_0 gives 1.9242027 radians. The solution was stable to a few parts per million over the duration of the test run.

The Euler angles of the subsatellite should be constant with respect to a reference frame rotating with the Shuttle. The integration is done in terms of direction cosines instead of angles. The direction cosines are converted to Euler angles at each output point. In order to check the orientation of the subsatellite in the rotating reference frame, the direction cosine matrix can be rotated by the negative of the orbital angle and then converted to Euler angles. In the test case, since the orbital motion is in the x-y plane, the rotated matrix is

$$\begin{bmatrix} \alpha_1 & \beta_1 & \gamma_1 \\ \alpha_2 & \beta_2 & \gamma_2 \\ \alpha_3 & \beta_3 & \gamma_3 \end{bmatrix} \cdot \begin{bmatrix} \cos & -\sin & 0 \\ \sin & \cos & 0 \\ 0 & 0 & 1 \end{bmatrix}$$

where Ω is the orbital angle.

When this transformation is applied in the program, the angle ψ is constant during the first 300 sec to an accuracy of a few parts per million (see Figure 3-2).

ORIGINAL PAGE IS
OF POOR QUALITY

0.0 0.349065594E+00
 10.0 0.349065916E+00
 20.0 0.349065893E+00
 30.0 0.3490658813E+00
 40.0 0.3490658478E+00
 50.0 0.3490657969E+00
 60.0 0.3490657551E+00
 70.0 0.349065717E+00
 80.0 0.349065684E+00
 90.0 0.349065665E+00
 100.0 0.3490656107E+00
 110.0 0.3490655865E+00
 120.0 0.3490655799E+00
 130.0 0.3490655688E+00
 140.0 0.3490655592E+00
 150.0 0.3490655448E+00
 160.0 0.3490655285E+00
 170.0 0.349065512E+00
 180.0 0.349065496E+00
 190.0 0.349065480E+00
 200.0 0.3490654630E+00
 210.0 0.349065447E+00
 220.0 0.3490670036E+00
 230.0 0.3490667744E+00
 240.0 0.3490669284E+00
 250.0 0.3490666684E+00
 260.0 0.3490665702E+00
 270.0 0.3490665557E+00
 280.0 0.3490665967E+00
 290.0 0.349066559E+00
 300.0 0.3490669747E+00

t
θ
(seconds) (radians)

Figure 3-2. Spinning Subsattellite Stable Configurations. Software Test Case (a) DUMBEL: 0 vs. Time.

ORIGINAL PAGE IS
OF POOR QUALITY

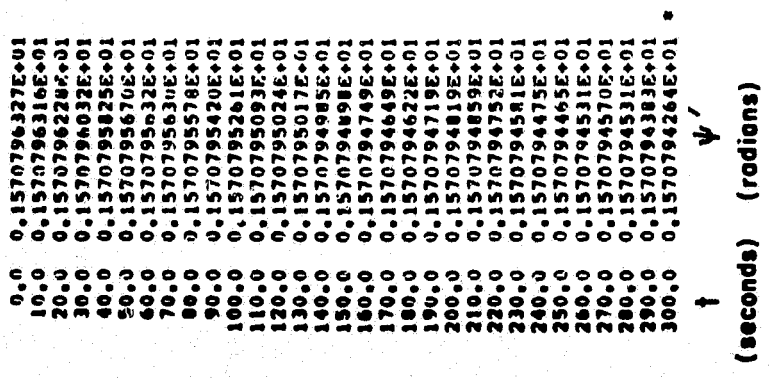


Figure 3-2 (cont.). (b) DUMBEL: ψ' vs. Time (ψ' is in Rotating Co-ordinate System).

ORIGINAL PAGE IS
OF POOR QUALITY

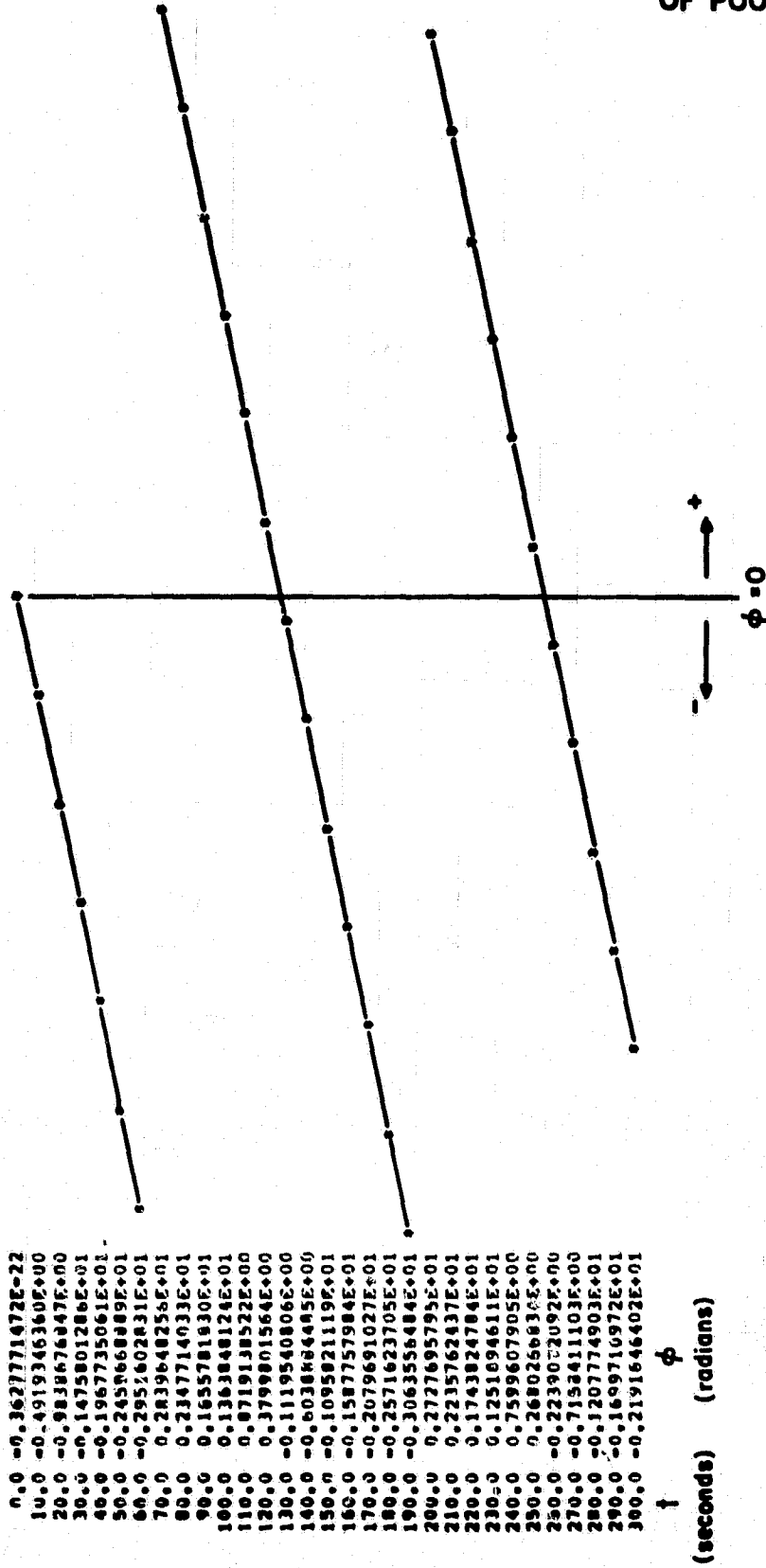


Figure 3.2 (cont.). (c) DUMBEL: ϕ vs. Time.

3.2 Multiple-Mass Tether Model (SKYHOOK)

3.2.1 SKYHOOK Tether Model with Subsatellite Rotational Dynamics Capability

The SKYHOOK computer program has been modified to include the rotation of the subsatellite using the method of direction cosines as defined in Annex III of the report "Study of the Dynamics of a Tethered Satellite System (SKYHOOK)," Kalaghan et al. March 1978 (see Appendix). The angular damping described in Annex III has not been included in SKYHOOK. The inclusion of rotational dynamics involved changing five of the existing routines in Skyhook and adding six new routines. The modified routines are the main program SKYHOOK, and subroutines MASSPTY, SKYIN2, DIFFUN, and TENSION. The new routines are DIFROT, ANGOUT, CROSS, ATTACHP, GROTAT, and PROTAT. The input to the program has been changed to read the number of rotational equations (either 12 or 0), the initial values of the rotational state vector, the vector from the center of mass to the attachment point of the tether, and the three moments of inertia about the principle axes of the subsatellite.

The format for reading the initial conditions for the rotational dynamics follows the general philosophy used in Skyhook of keeping the input as general as possible. The user is expected to generate the initial conditions with a preprocessor designed for the particular problem to be studied. At SAO the initial conditions are generated using a small program called DUMBEL. The version of DUMBEL which models the rotational dynamics reads the Euler angles and their derivatives as the initial conditions. The program then calculates direction cosines and angular velocities using the equations on page 13 of Annex III. The initial position and velocity for the Shuttle and subsatellite are computed in DUMBEL from the orbital parameters given on input. The state vector for the Shuttle consists of six quantities. The total state vector for the subsatellite consists of 18 quantities. The state vectors for each vehicle are written onto a file

in the format for input to the SKYHOOK program. In order to have the system in tension equilibrium, the offset of the center of gravity from the attachment point must be taken into account. This is done by computing the offset in the inertial coordinate system and using this vector to offset the center of gravity from the attachment point so that the distance from the Shuttle to the attachment point is equal to the tether length specified on input.

The following paragraphs describe the changes made to each of the five routines that have been changed in Skyhook.

Three changes have been made in the main program SKYHOOK. Some quantities have been added to the labelled common block MASSES which occurs in the routines SKYHOOK, MASSPTY, SKYIN2, and DIFFUN. These quantities are NROTEQ (the number of rotational equations), ATTACH (3) (the vector from the center of mass to the attachment point in the body fixed coordinates), XINERT(3) (the moment of inertia about each of the principle axes), ROTMAT (3,3) (the direction cosine matrix), ANGVEL(3) (the angular velocity about each of the body axes), and ANG(3) (the Euler angles in inertial coordinates). The other changes involve the deployment mode of the program. If rotational dynamics is being included, the initial conditions for the subsatellite must be taken from input rather than being obtained from subroutine INITAL which sets up initial conditions for new masses to be deployed.

The changes in MASSPTY consist of adding the new quantities to the common block MASSES and processing the additional input data needed for modelling the rotation of the subsatellite. The number of rotational equations NROTEQ is read, printed and added to the number of equations to be integrated for the subsatellite. Initial conditions for the subsatellite are read from input in the deployment mode when rotational dynamics is included. The point of attachment and moments of inertia are read and printed.

The following changes have been made to SKYIN2. The new quantities have been added to the MASSES common block as described in the paragraph on the main program SKYHOOK. Two vectors have been added providing information used by the numerical integrator. The vector ZMAXR(12) gives the maximum value of the twelve rotational quantities, and PEROT(12) gives the increment to be used for numerical differentiation in subroutine FEDERV. These vectors are inserted into the arrays ZMAX and PEDINC by a new routine PROTAT. A new subroutine ANGOUT is called by SKYIN2 to compute and print the Euler angles from the direction cosine matrix. The Euler angles have also been added to the output on unit 7 which is used by the plotting routines.

Subroutine DIFFUN computes the rate of change of each variable to be integrated by the numerical integrator. The following changes have been made. The new rotational quantities have been added to the common block MASSES. The new routine GROTAT is called to get the rotational state vector from the master array. The arrays ATTACH, ROTMAT, and ANGVEL have been added to the call to TENSION which computes the wire tension. A new routine DIFROT is called to return the rate of change of the rotational quantities and the results are placed in the array DZ by a new subroutine PROTAT.

Subroutine TENSION has been modified to compute the tension from the position and velocity of the point of attachment of the wire rather than from the center of mass of the subsatellite. The arrays ATTACH, ROTMAT, and ANGVEL have been added to the calling sequence. A new routine ATTACHP is called to compute the position and velocity of the point of attachment of the wire on the subsatellite. The tension is computed from the difference in position and velocity between the attachment and the neighboring mass point.

The following six paragraphs describe the new routines that have been added to SKYHOOK for including the rotational dynamics of the subsatellite.

The rate of change of each quantity in the rotational state vector is computed by subroutine DIFROT (ATTACH,ROTMAT,ANGVEL,FTENS,XINERT,DD,IM,BMASS), where ATTACH is the offset of the attachment point of the tether from the center of mass of the subsatellite, ROTMAT is the direction cosine matrix, ANGVEL is the vector angular velocity with respect to the body axes, FTENS is the acceleration due to the wire tension, XINERT is the vector giving the moments of inertia about the principle axes, DD is the output vector giving the rate of change of each quantity, IM is the mass number (which must be 2 or the subroutine returns zero), and BMASS is the subsatellite mass used to compute the wire tension from the acceleration FTENS. The subroutine computes the force on the subsatellite due to the wire tension in the body axis coordinate system. This is then used to compute the components of the torque along each body axis. The rate of change of each of the 12 quantities in the state vector is computed using the equations on page 12 of Annex III.

The Euler angles corresponding to the direction cosine matrix are computed and printed by subroutine ANGOUT(TOUT,ZOUT,IPT,NTEQ,NEDEQ,NROTEQ,ANG) where TOUT is the time in seconds, ZOUT is the total state vector, IPT is a vector giving the state of each mass point in the ZOUT array, NTEQ is the number of temperature equations, NEDEQ is the number of electrodynamic equations, NROTEQ is the number of rotational equations for the subsatellite, and ANG is the vector of Euler angles. The Euler angles are computed using the equations on pages 13 and 14 of Annex III.

Subroutine CROSS(A,B,C) computes C as the cross product of A and B.

The position and velocity of the attachment point of the tether on the subsatellite is computed by subroutine ATTACHP(ATTACH,ROTMAT,ANGVEL,SV,SVP,IM) where ATTACH, ROTMAT, and ANGVEL have been previously defined, SV is the state vector of the center of mass, SVP is the state vector of the

attachment point, and IM is the mass number. If IM is not 2, SVP equals SV. The position of the attachment point is obtained by rotating ATTACH using the rotation matrix ROTMAT and adding the result to the positional part of SV. The velocity of the attachment point is obtained by taking the cross product of ANGVEL and ATTACH and adding the result to the velocity components of SV. The cross product is performed after rotating ANGVEL and ATTACH to inertial coordinates.

The rotational state vector is extracted from the total state vector of the system by subroutine GROTAT(A,NDIM,IPT,NTEQ,NEDEQ,NROTEQ,ROTMAT,ANGVEL) where A is the total state vector for all masses, NDIM is the number of rows in the matrix A, IPT is the vector of indices giving the starting location for each mass, NTEQ is the number of temperature equations, NEDEQ is the number of electrodynamic equations, NROTEQ is the number of rotational equations for the subsatellite, ROTMAT is the matrix of direction cosines, and ANGVEL is the angular velocity vector.

The rotational state vector is placed in the total state vector array by subroutine PROTAT(A,NDIM,IPT,NTEQ,NEDEQ,NROTEQ,DD) where the quantities are the same as described in the last paragraph for subroutine GROTAT. The vector DD is of length 12 and includes both the direction cosines and angular velocity components.

3.2.2 Testing of SKYHOOK with Rotational Dynamics

The new version of the SKYHOOK program with rotational dynamics has been tested using the special case of Section 2.0 used previously to test the two-mass (DUMBEL) model. The initial rotational state vector from DUMBEL has been used as input to the SKYHOOK program. In testing the program it is helpful to plot the Euler angles to see how they change with time. The DUMBEL program includes a facility for generating printer page plots of various

quantities vs. time. The Euler angles were plotted using this facility when the special test case was run on the program. A similar facility exists for plotting the quantities written on unit 7 by the SKYHOOK program. This utility program has been modified to include plots of the Euler angles which have been added to the SKYHOOK program output. The SKYHOOK program has been tested by running the test case on SKYHOOK and comparing the plots from SKYHOOK with those of DUMBEL. After correction of various bugs, agreement was obtained between the two programs. For the test case, the angle θ is constant with time and the angle ψ increases at a rate equal to the orbital angular velocity (compare Figure 3-3 with Figure 3-2). The angular velocity $\dot{\phi}$ is constant.

3.3 Behavior of a Subsatellite with a Single Thruster

A simple test case has been run as an example of a rotational dynamics simulation with an attitude thruster. The system is assumed to be initially in equilibrium with the subsatellite hanging at rest at the end of the tether with no angular velocity except that of the orbital motion. At $t = 0$ an attitude thruster applies a constant torque about the body axis which is aligned with the tether. The parameters of the run are mostly the same as those used in the test case described in Section 3.1.2. For the thruster case the initial conditions are $\theta_0 = \psi_0 = 90^\circ$, $\dot{\phi}_0 = 1.178 \times 10$ rad/sec (the orbital angular velocity), and $\dot{\theta}_0 = \dot{\psi}_0 = 0$. The Euler angles θ and ψ are shown in Figure 2-1. The torque has been chosen to be 4×10^8 dyne-cm which would result in an angular velocity of .1 radians/sec in 500 seconds with a moment of inertia of 2×10^{12} (cgs). A slow acceleration allows the orbital angle to change significantly before the spin rate has reached a value which would cause slow numerical integration. Since the equations of motion are written as a function of the components of the torque about

ORIGINAL PAGE IS
OF POOR QUALITY

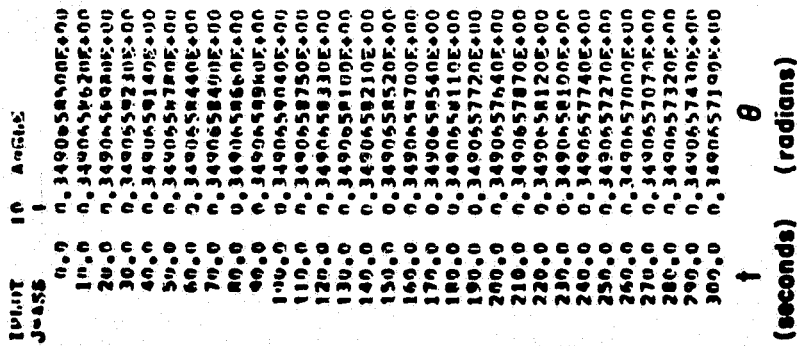


Figure 3-3. Spinning Subsatellite Stable Configuration. Software Test Case (a) SKYHOOK: θ vs. Time.

ORIGINAL PAGE IS
OF POOR QUALITY

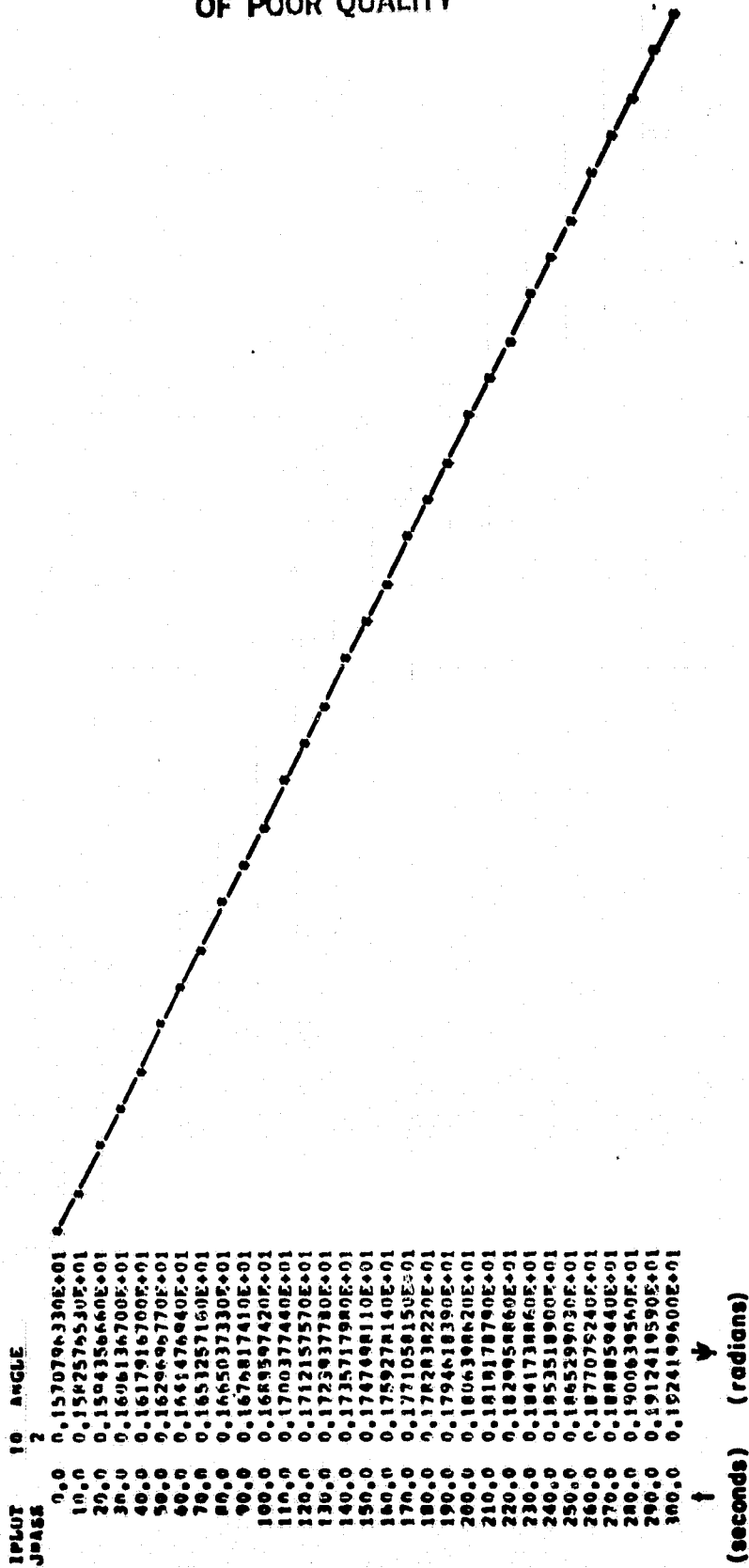


Figure 3-3 (cont.). (b) SKYHOOK: ψ vs. Time (ψ is in Inertial Co-ordinate System which Results in Linear Increase of ψ with Time).

ORIGINAL PAGE IS
OF POOR QUALITY

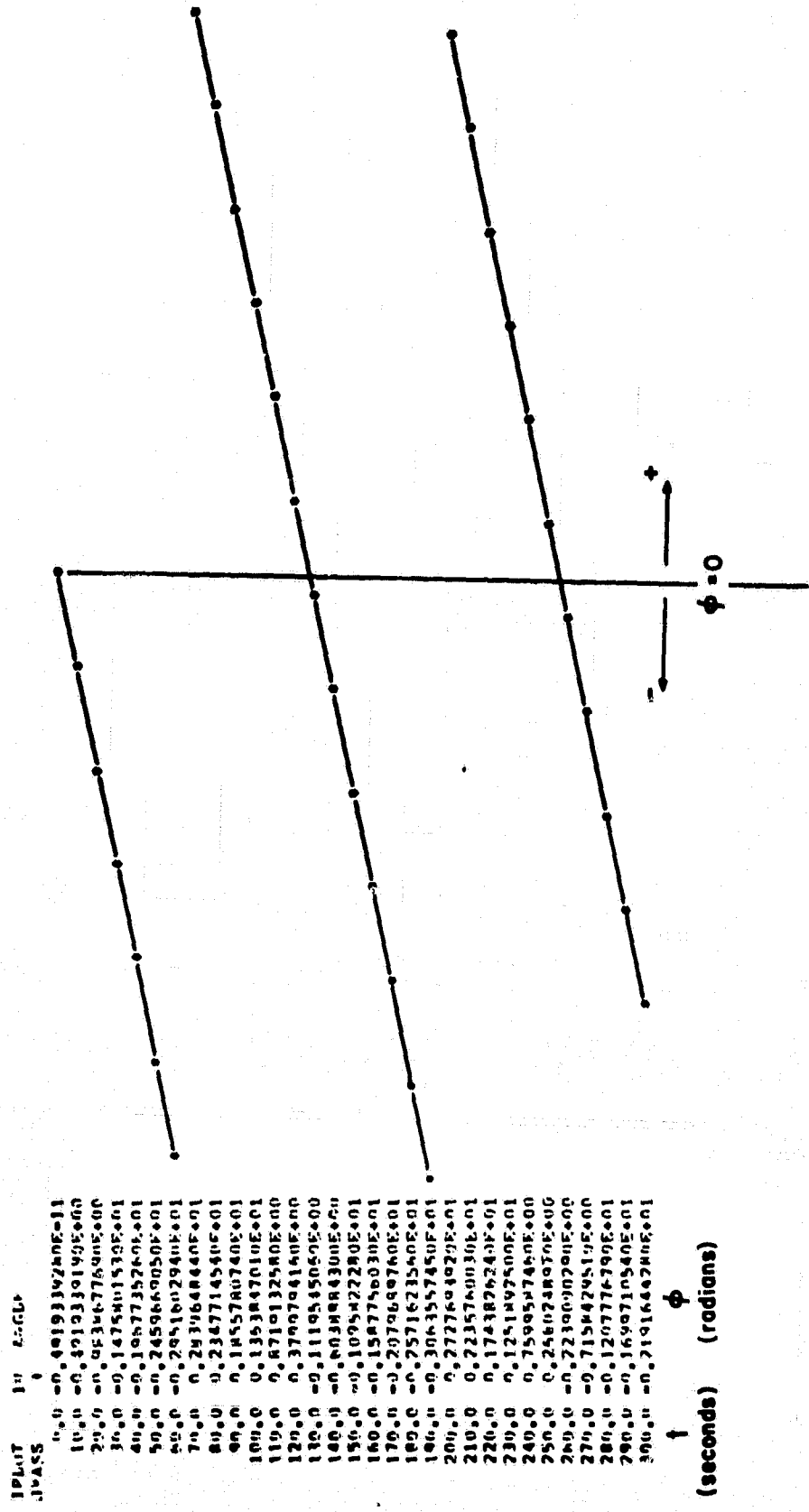


Figure 3-3 (cont.). (c) SKYHOOK: ϕ vs. Time.

the body axes, this case can be implemented by adding a constant to the torque about the body z axis. The only other torque currently modelled in the program is that of the wire tension.

The thruster case described above has been run on both the DUMBEL program and the SKYHOOK program. The initial rotational state vector generated by DUMBEL has been used as input to the SKYHOOK program. In each program the thruster model was implemented by adding a constant torque about the body z axis. The Euler angles have been plotted using the printer page as a graph. The output from DUMBEL differs from that of SKYHOOK in that the Euler angles are referred to a rotating orbital coordinate system. This affects only the angle ψ since the orbit is equatorial. The difference between the plots from the two programs was helpful for the thruster case since the angle ψ is initially constant in the rotating frame and then stops moving with the orbit and becomes nearly constant in the inertial frame as the spin increases.

Figure 3-4 shows the Euler angles vs. time for the simple thruster case as run in the SKYHOOK program. Part a) is the inclination angle θ , part b) is the nodal angle ψ , and part c) is the spin angle ϕ about the principle axis. Initially, the rate of change of ψ is equal to the orbital angular velocity. In the output of the DUMBEL program the angle ψ was initially constant in the rotating orbital reference frame. As the subsatellite begins to spin up, the nodal rotation is arrested as can be seen in part b) of the plot. Once the node stops rotating, the tether force \vec{F} is no longer aligned with the vector \vec{r} from the center of mass to the attachment point, so there is a torque on the subsatellite. In Figure 3-5 we see that the torque $\vec{\tau}$ is directed toward the +z axis. Since the angular velocity is in the direction of \vec{r} , the torque will cause the principle axes to move up out of the x-y plane, thereby decreasing the angle θ as seen in part a)

ORIGINAL PAGE IS
OF POOR QUALITY

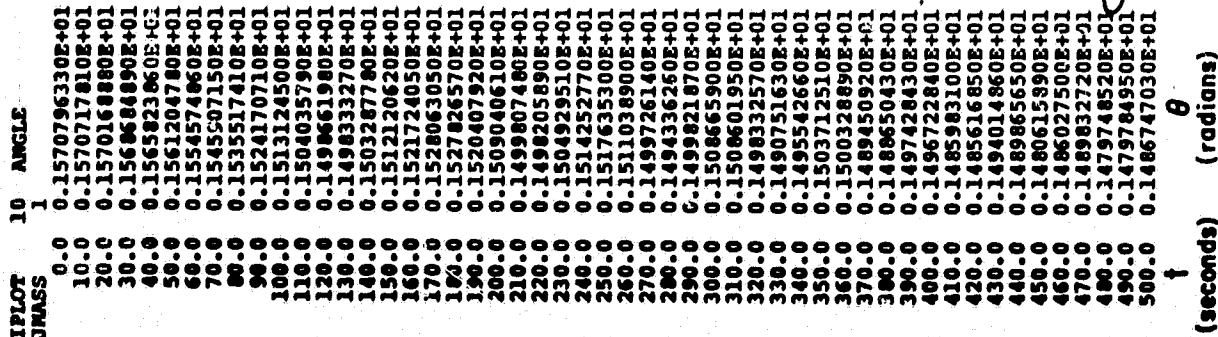


Figure 3-4. Attitude Thruster Test Case (a) Inclination Angle (θ) vs. Time.

ORIGINAL PAGE IS
OF POOR QUALITY

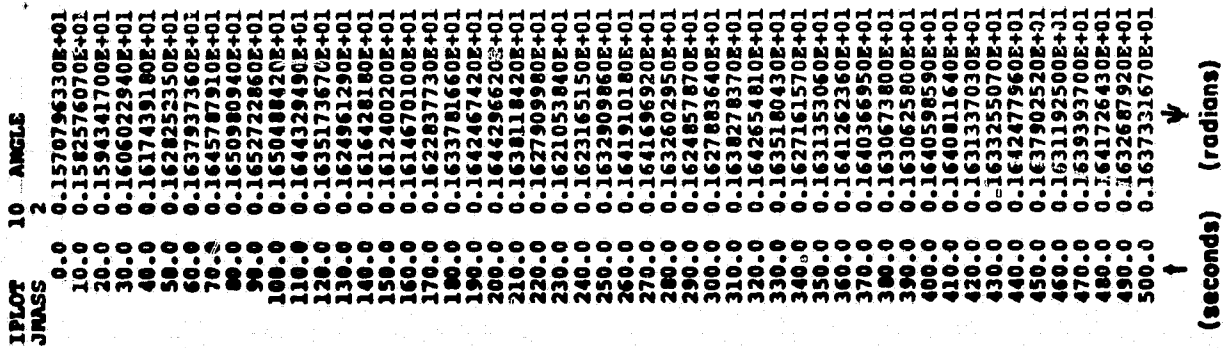


Figure 3-4 (cont.). (b) Nodal Angle ψ vs. Time.

ORIGINAL PAGE IS
OF POOR QUALITY

IPL	JRASS	10 ANGLE
0.0	0.0	0.100000000E-23
10.0	0.999768770E-02	0.0
20.0	0.399963083E-01	0.0
30.0	0.8998146200E-01	0.0
40.0	0.1599426250E+00	0.0
50.0	0.249859350E+00	0.0
60.0	0.3597434190E+00	0.0
70.0	0.4895849550E+00	0.0
80.0	0.6394120390E+00	0.0
90.0	0.8093643710E+00	0.0
100.0	0.9994848060E+00	0.0
110.0	0.1209871970E+01	0.0
120.0	0.1440511750E+01	0.0
130.0	0.1691254070E+01	0.0
140.0	0.1961855600E+01	0.0
150.0	0.2252114660E+01	0.0
160.0	0.2561997960E+01	0.0
170.0	0.2891629330E+01	0.0
180.0	-0.3042017800E+01	0.0
190.0	-0.2672415540E+01	0.0
200.0	-0.2282509330E+01	0.0
210.0	-0.1872091960E+01	0.0
220.0	-0.1441351760E+01	0.0
230.0	-0.990697200E+00	0.0
240.0	-0.5209907710E+00	0.0
250.0	-0.3151597270E-01	0.0
260.0	0.4779963490E+00	0.0
270.0	0.1008011060E+01	0.0
280.0	0.1556691640E+01	0.0
290.0	0.2129271760E+01	0.0
300.0	0.2719080430E+01	0.0
310.0	-0.2954739340E+01	0.0
320.0	-0.2325021220E+01	0.0
330.0	-0.1674439510E+01	0.0
340.0	-0.1003806320E+01	0.0
350.0	-0.3140930580E+00	0.0
360.0	0.3952391250E+00	0.0
370.0	0.1125321180E+01	0.0
380.0	0.1876125570E+01	0.0
390.0	0.2646141380E+01	0.0
400.0	-0.2847764540E+01	0.0
410.0	-0.2037766060E+01	0.0
420.0	-0.1206947870E+01	0.0
430.0	-0.3570899780E+00	0.0
440.0	0.5121989320E+00	0.0
450.0	0.1402606050E+01	0.0
460.0	0.2313206140E+01	0.0
470.0	-0.3040643230E+01	0.0
480.0	-0.2090826370E+01	0.0
490.0	-0.1113989410E+01	0.0
500.0	-0.1303807260E+00	0.0

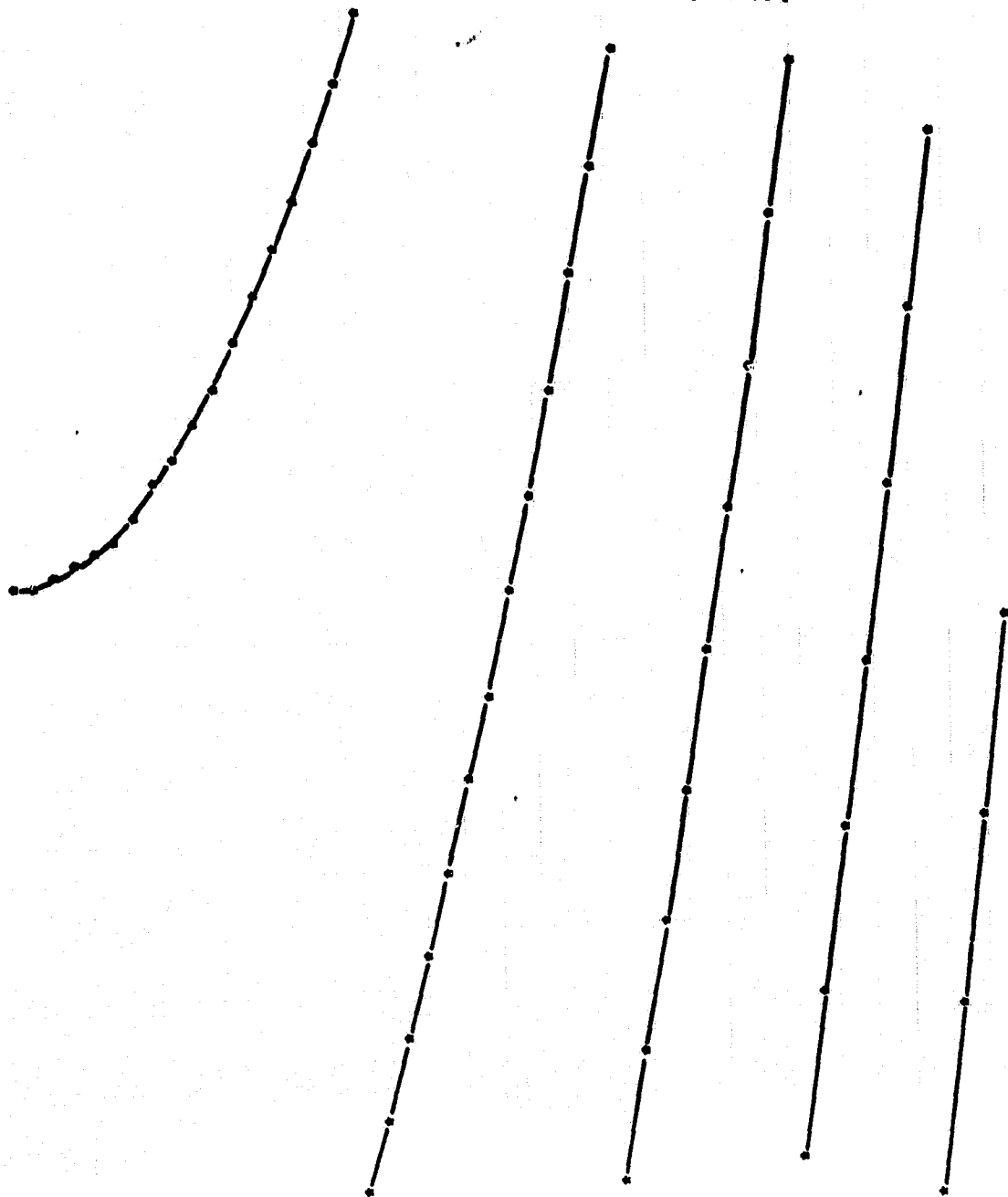


Figure 3-4 (cont.). (c) Spin Angle ϕ vs. Time.

of Figure 3-4. The angle ϕ circulates with increasing angular velocity as seen in part c) of Figure 3-4. The angle has not been normalized to a continuous variable so that there is a discontinuity every time the angle passes 180 degrees.

4.0 Adaptation of SKYHOOK General Rotational Dynamics Model to Specific Attitude Control Systems

The SKYHOOK program now provides a basic tool for studying the dynamics of the tether system including the rotation of the subsatellite. It remains only to develop suitable models for "real-world" attitude control systems to convert their input forces and torques into parameters directly readable by SKYHOOK. The implementation of such models would be done by means of routines that compute the torque on the subsatellite as a function of the observables available in the program. This torque would be added to the torque from the wire and the result used in the equations of motion which have been incorporated in the program for integrating the rotation of the subsatellite. Routines would be developed for each of the various attitude control systems such as thrusters, magnetic torquers, etc. These routines are straightforward and do not represent a major development effort.

ORIGINAL PAGE IS
OF POOR QUALITY

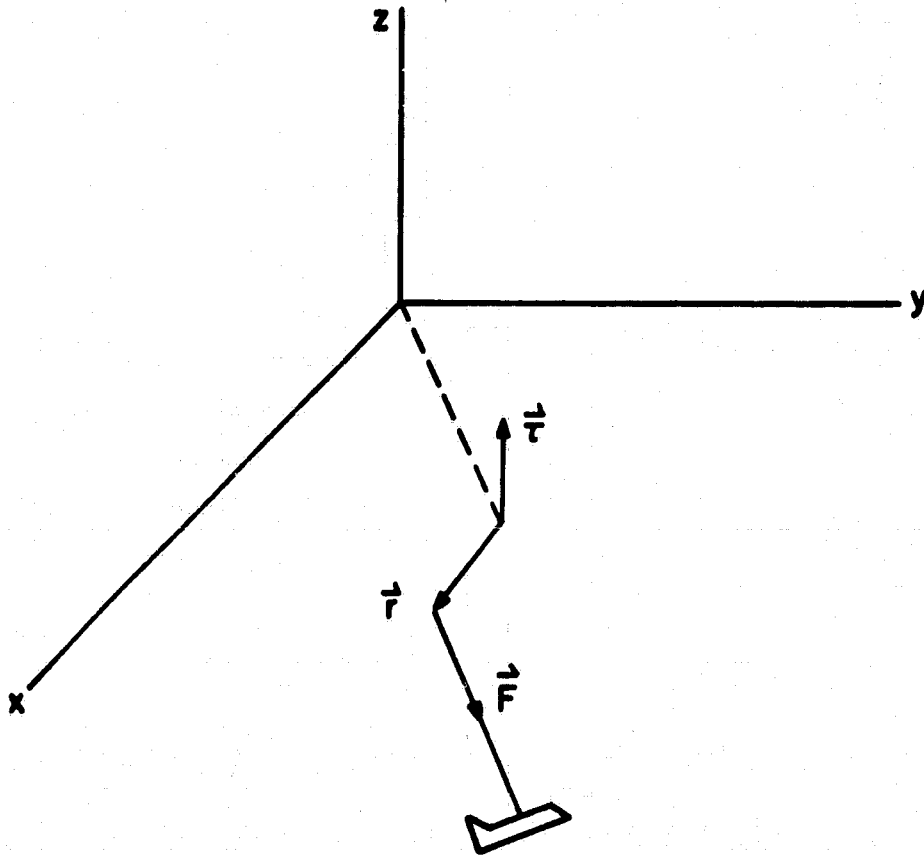


Figure 3-5. Subsatellite Torque Vector Conventions.

APPENDIX

**ROTATIONAL DYNAMICS OF
SUBSATELLITE VEHICLE**

ROTATIONAL DYNAMICS OF SUBSATELLITE VEHICLE

III-1. EQUATIONS OF MOTION OF THE DUMBBELL SYSTEM WITH A RIGID BODY AT ONE END

The short dumbbell program integrates the motion of two vehicles connected by a massless tether. One vehicle is treated as a point mass and the other is treated as a rigid body attached to the tether. Two types of damping are included: The first is proportional to the rate of change of the distance between the two vehicles, while the second consists of angular damping at the point of suspension of the rigid body. The program has facilities for computing the initial state vector of the system from parameters specifying the desired orbital and system characteristics. The wire parameters necessary to achieve the desired initial conditions and the damping constants required for critical damping of the spring oscillations and angular oscillations of the end mass are also calculated.

III-1.1 Calculation of the Initial State Vector

A single particle in a circular orbit in an inverse-square force field obeys the equation

$$\frac{GMm}{r^2} = m r \omega^2$$

or

$$GM = r^3 \omega^2 ,$$

where G is the gravitational constant, M is the mass of the central body, m is the mass of the particle, r is the radius of the orbit, and ω is the angular velocity of the particle.

A similar equation can be written for two particles of mass m_1 and m_2 in circular orbits of radius r_1 and r_2 connected by a massless tether. Assuming $r_2 > r_1$, the particles obey the simultaneous equations

$$\frac{GM m_1}{r_1^2} - T = m_1 r_1 \omega^2$$

and

$$\frac{GM m_2}{r_2^2} + T = m_2 r_2 \omega^2 ,$$

which can be solved to obtain the angular velocity ω and the wire tension T . We can eliminate T by adding the equations. This gives the equation

$$GM \left(\frac{m_1}{r_1^2} + \frac{m_2}{r_2^2} \right) = (m_1 r_1 + m_2 r_2) \omega^2$$

or

$$GM = \frac{m_1 r_1 + m_2 r_2}{(m_1/r_1^2) + (m_2/r_2^2)} \omega^2 .$$

Comparing this to the equation for a single particle, we see that the system orbits like a single particle in an orbit of radius \bar{r} given by

$$\bar{r}^3 = \frac{m_1 r_1 + m_2 r_2}{(m_1/r_1^2) + (m_2/r_2^2)} .$$

The equation for the angular velocity is

$$\omega = \sqrt{\frac{GM}{\bar{r}^3}} .$$

Solving for the tension, we obtain

$$T = GM \frac{(r_2/r_1^2) - (r_1/r_2^2)}{(r_1/m_2) + (r_2/m_1)} .$$

The velocities of the particles are

$$v_1 = r_1 \omega$$

and

$$v_2 = r_2 \omega .$$

The initial state vector for particles in circular orbits starting out on the x axis with inclination I is

$$\begin{aligned} x_1 &= r_1 , & \dot{x}_1 &= 0 , \\ y_1 &= 0 , & \dot{y}_1 &= v_1 \cos I , \\ z_1 &= 0 , & \dot{z}_1 &= v_1 \sin I , \\ x_2 &= r_2 , & \dot{x}_2 &= 0 , \\ y_2 &= 0 , & \dot{y}_2 &= v_2 \cos I , \\ z_2 &= 0 , & \dot{z}_2 &= v_2 \sin I . \end{aligned}$$

If a slight eccentricity e is desired in the orbit, we can obtain an initial state vector from the following simple approximation. In polar coordinates, the equation of an ellipse is given by

$$r = \frac{a(1 - e^2)}{1 + e \cos(\theta - \theta_0)} ,$$

where a is the semimajor axis. Differentiating with respect to time, we have

$$\dot{r} = \frac{a(1 - e^2) e \sin(\theta - \theta_0) \dot{\theta}}{[1 + e \cos(\theta - \theta_0)]^2} .$$

If $e \ll 1$, the maximum value of \dot{r} is approximately

$$\dot{r}_{\max} = ae\dot{\theta} .$$

ORIGINAL PAGE IS
OF POOR QUALITY

Therefore, we can obtain a small eccentricity in the orbit by setting $\dot{x}_1 = \dot{x}_2 = \bar{r}\omega$ in the initial state vector.

III-1.2 Calculation of the Wire Constants

The cross-section area A of a wire of diameter D is

$$A = \pi \left(\frac{D}{2}\right)^2 .$$

If the natural length of the wire is l_0 and the elasticity is E , the spring constant k is

$$k = \frac{EA}{l_0} .$$

When the distance between the ends of the wire is l , the tension T is

$$\begin{aligned} T &= k(l - l_0) , & l > l_0 , \\ &= 0 , & l < l_0 . \end{aligned}$$

For a dumbbell system starting out with an initial separation l and tension T , the natural length of the wire is calculated from

$$T = k(l - l_0) = \frac{EA}{l_0} (l - l_0) .$$

Solving for l_0 , we get

$$l_0 = \frac{l}{1 + (T/EA)} .$$

III-1.3 Critical Damping for the Dumbbell System

The dumbbell system shown in Figure 1 oscillates about its center of mass (CM).

ORIGINAL PAGE IS
OF POOR QUALITY

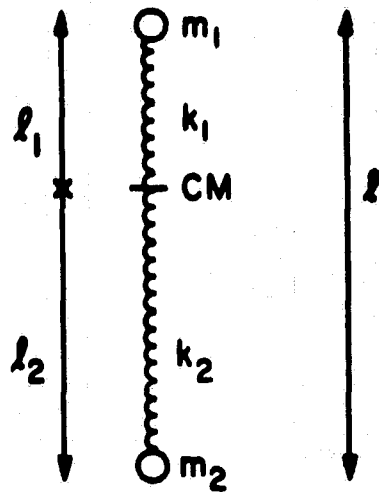


Figure 1.

The distances of each particle from the CM are

$$l_1 = \frac{m_2 l}{m_1 + m_2} ,$$

and

$$l_2 = \frac{m_1 l}{m_1 + m_2} .$$

If the spring constant of the entire length is k , the spring constants of each section are

$$k_1 = k \frac{l}{l_1} = k \frac{m_1 + m_2}{m_2} ,$$

and

$$k_2 = k \frac{m_1 + m_2}{m_1} .$$

The equation of motion for each section with damping is

$$m_1 \ddot{\theta}_1 + b_1 \dot{\theta}_1 + k_1 \theta_1 = 0 \quad ,$$

where b_1 is the damping constant. For critical damping, the determinant of the characteristic equation is zero, which gives

$$\sqrt{b_1^2 - 4 m_1 k_1} = 0$$

or

$$b_1 = 2 \sqrt{m_1 k_1} \quad .$$

The damping term $b_1 \dot{\theta}_1$ can be rewritten in terms of $\dot{\theta}$ to give

$$\begin{aligned} b_1 \dot{\theta}_1 &= \left(2 \sqrt{m_1 k_1} \right) \left(\frac{m_j \dot{\theta}}{m_1 + m_j} \right) \quad , \quad i \neq j \\ &= \left(2 \sqrt{m_1 k \frac{m_1 + m_j}{m_j}} \right) \left(\frac{m_j \dot{\theta}}{m_1 + m_j} \right) \\ &= 2 \sqrt{k \frac{m_1 m_j}{m_1 + m_j}} \dot{\theta} \quad . \end{aligned}$$

Therefore, the damping force can be written as $b \dot{\theta}$, where b is defined as

$$b = 2 \sqrt{k \frac{m_1 m_2}{m_1 + m_2}} \quad .$$

III-1.4 Critical Damping for Angular Oscillations

A simple pendulum with angular damping executing small oscillations obeys the equation

$$I\ddot{\theta} + b\dot{\theta} + Tr\theta = 0 ,$$

where I is the moment of inertia, b is the angular damping constant, T is the vertical force on the pendulum, r is the length of the pendulum, and θ is the angular rotation of the pendulum from equilibrium. The characteristic equation obtained by substituting the solution

$$\theta = A e^{at}$$

is

$$Ia^2 + ba + Tr = 0 ,$$

which has the solution

$$a = \frac{-b \pm \sqrt{b^2 - 4ITr}}{2I} .$$

To obtain critical damping, the radical is set equal to zero, giving

$$b^2 - 4ITr = 0$$

or

$$b = 2\sqrt{ITr} .$$

This value of b can be used efficiently to damp out certain oscillations of the rigid body at one end of the dumbbell system. If the rigid body is not symmetric about the point of attachment, the damping constant cannot provide critical damping for both moments of inertia simultaneously. Motions that do not change the angle between r and T will not be damped. It is assumed that the last section of wire is rigid in order to provide a torque for the damping to work against.

Figure 2 shows a dumbbell system with a rigid body at one end. In the diagram, \vec{p}_1 is the position of the center of mass of the rigid body, \vec{p}_2 is the point of attachment

ORIGINAL PAGE IS
OF POOR QUALITY

of the wire, \vec{p}_3 is the position of the point mass, M is the mass of the rigid body, m is the mass of the point mass, \vec{r} is the vector from \vec{p}_1 to \vec{p}_2 , \vec{F} is the wire force acting on \vec{p}_2 , and θ is the angle between \vec{r} and \vec{F} .

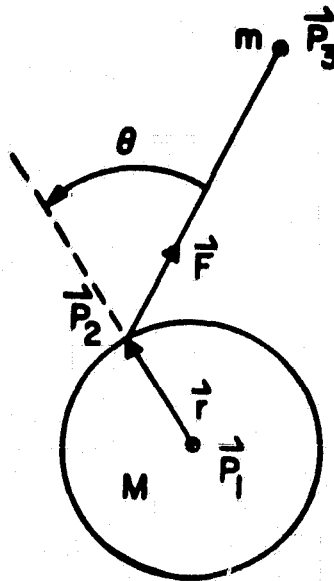


Figure 2.

The force \vec{F} is given by

$$\vec{F} = [k(l - l_0) + bl] \frac{\vec{p}_3 - \vec{p}_2}{l},$$

where $l = |\vec{p}_3 - \vec{p}_2|$. The derivative of l is given by

$$\begin{aligned} \dot{l} &= \frac{d}{dt} \sqrt{(\vec{p}_3 - \vec{p}_2) \cdot (\vec{p}_3 - \vec{p}_2)} = \frac{1}{2} l^{-1} [2(\dot{\vec{p}}_3 - \dot{\vec{p}}_2) \cdot (\vec{p}_3 - \vec{p}_2)] \\ &= \frac{(\dot{\vec{p}}_3 - \dot{\vec{p}}_2) \cdot (\vec{p}_3 - \vec{p}_2)}{l}. \end{aligned}$$

The equations of motion of \vec{p}_1 and \vec{p}_3 are

$$\vec{F} = M \ddot{\vec{p}} \quad \text{and} \quad -\vec{F} = m \ddot{\vec{p}}_3 ,$$

while the equation of motion for the angular momentum is

$$\dot{\vec{N}} = \dot{\vec{L}} ,$$

where \vec{L} is the angular momentum and \vec{N} , the applied torque, is

$$\vec{N} = \vec{N}_W + \vec{N}_D ,$$

in which the wire torque is $\vec{N}_W = \vec{r} \times \vec{F}$. The damping torque \vec{N}_D is parallel to \vec{N}_W if $\vec{N}_W \neq 0$ or parallel to $\hat{p} \times \hat{F} + \hat{p} \times \hat{F}$ if $\vec{N}_W = 0$.

The applied force \vec{F} is

$$\vec{F} = T \hat{F} ,$$

where T is the tension in the wire and

$$\hat{F} = \frac{\vec{p}_3 - \vec{p}_2}{|\vec{p}_3 - \vec{p}_2|} ,$$

where $\vec{p}_2 = \vec{p}_1 + \vec{r}$.

The damping torque is

$$\vec{N}_D = b\dot{\theta} \frac{\vec{r} \times \vec{F}}{|\vec{r} \times \vec{F}|} .$$

The quantity $\dot{\theta}$ can be obtained from differentiating either

ORIGINAL PAGE IS
OF POOR QUALITY

$$\cos \theta = \hat{\mathbf{r}} \cdot \hat{\mathbf{F}} ,$$

or

$$\sin \theta = |\hat{\mathbf{r}} \times \hat{\mathbf{F}}| ,$$

where

$$\hat{\mathbf{r}} = \frac{\mathbf{r}}{|\mathbf{r}|} , \quad \hat{\mathbf{F}} = \frac{\mathbf{F}}{|\mathbf{F}|} .$$

Using the $\cos \theta$ expression, we have

$$\frac{d}{dt} (\cos \theta) = \frac{d}{dt} (\hat{\mathbf{r}} \cdot \hat{\mathbf{F}}) ,$$

$$-\dot{\theta} \sin \theta = \dot{\hat{\mathbf{r}}} \cdot \hat{\mathbf{F}} + \hat{\mathbf{r}} \cdot \dot{\hat{\mathbf{F}}} ,$$

$$\dot{\theta} = - \frac{\dot{\hat{\mathbf{r}}} \cdot \hat{\mathbf{F}} + \hat{\mathbf{r}} \cdot \dot{\hat{\mathbf{F}}}}{|\hat{\mathbf{r}} \times \hat{\mathbf{F}}|} .$$

The above formula is not good near $\theta = 0^\circ$ and 180° , for which we use

$$\frac{d}{dt} (\sin \theta) = \frac{d}{dt} |\hat{\mathbf{r}} \times \hat{\mathbf{F}}| ,$$

$$\dot{\theta} \cos \theta = \frac{d}{dt} [(\hat{\mathbf{r}} \times \hat{\mathbf{F}}) \cdot (\hat{\mathbf{r}} \times \hat{\mathbf{F}})]^{1/2} ,$$

$$\dot{\theta} \times \hat{\mathbf{r}} \cdot \hat{\mathbf{F}} = \frac{1}{2} \frac{1}{|\hat{\mathbf{r}} \times \hat{\mathbf{F}}|} \left[2\hat{\mathbf{r}} \times \dot{\hat{\mathbf{F}}} \cdot \frac{d}{dt} (\hat{\mathbf{r}} \times \hat{\mathbf{F}}) \right] ,$$

$$\dot{\theta} = \frac{1}{\hat{\mathbf{r}} \cdot \hat{\mathbf{F}}} \frac{\hat{\mathbf{r}} \times \dot{\hat{\mathbf{F}}}}{|\hat{\mathbf{r}} \times \hat{\mathbf{F}}|} \cdot (\hat{\mathbf{r}} \times \hat{\mathbf{F}} + \hat{\mathbf{r}} \times \dot{\hat{\mathbf{F}}}) .$$

For critical damping of simple pendulum motion, the damping constant b is

$$b = 2\sqrt{ITr} ,$$

where I is the moment of inertia, T is the tension, and r is the distance from the center of mass to the point of attachment. The quantity \hat{r} is given by

$$\hat{r} = \vec{\omega} \times \hat{r} ,$$

where $\vec{\omega}$ is the angular velocity of the subsatellite. The vector \hat{F} is given by

$$\hat{F} = \frac{1}{\Delta p} \left(\dot{\Delta p} - \Delta p \cdot \frac{\dot{\Delta p}}{|\Delta p|} \right) ,$$

where

$$\Delta p = \vec{p}_3 - \vec{p}_2 ,$$

$$\dot{\Delta p} = \dot{\vec{p}}_3 - \dot{\vec{p}}_2 ,$$

$$= \dot{\vec{p}}_3 - (\dot{\vec{p}}_1 + \dot{\vec{r}}) ,$$

$$= \dot{\vec{p}}_3 - (\dot{\vec{p}}_1 + \vec{\omega} \times \vec{r}) .$$

The vector \hat{r} is fixed with respect to the principal axes of the subsatellite. The orientation of the subsatellite with respect to a set of inertial space axes can be given by specifying the nine direction cosines that give the transformation from the space axes to the body axes. The components x , y , and z of a vector with respect to the inertial axes are thus related to the components, x' , y' , and z' with respect to the principal axes of the body by the matrix equation

$$\begin{pmatrix} x' \\ y' \\ z' \end{pmatrix} = \begin{pmatrix} \alpha_1 & \beta_1 & \gamma_1 \\ \alpha_2 & \beta_2 & \gamma_2 \\ \alpha_3 & \beta_3 & \gamma_3 \end{pmatrix} \begin{pmatrix} x \\ y \\ z \end{pmatrix} .$$

ORIGINAL PAGE IS
OF POOR QUALITY

The reverse transformation is

$$\begin{pmatrix} x \\ y \\ z \end{pmatrix} = \begin{pmatrix} a_1 & a_2 & a_3 \\ \beta_1 & \beta_2 & \beta_3 \\ \gamma_1 & \gamma_2 & \gamma_3 \end{pmatrix} \begin{pmatrix} x' \\ y' \\ z' \end{pmatrix} .$$

The components of the angular velocity $\vec{\omega}$ with respect to the principal axes are ω_1 , ω_2 , and ω_3 , and the principal moments of inertia are I_1 , I_2 , and I_3 . The components of \vec{L} with respect to the principal axes of the body are given by the Euler equations

$$\vec{N} = \dot{\vec{L}} = \begin{pmatrix} I_1 \dot{\omega}_1 - \omega_2 \omega_3 [I_2 - I_3] \\ I_2 \dot{\omega}_2 - \omega_3 \omega_1 [I_3 - I_1] \\ I_3 \dot{\omega}_3 - \omega_1 \omega_2 [I_1 - I_2] \end{pmatrix} .$$

The equations for the nine direction cosines are as follows:

$$\begin{aligned} \dot{a}_1 + \omega_2 a_3 - \omega_3 a_2 &= 0 , \\ \dot{a}_2 + \omega_3 a_1 - \omega_1 a_3 &= 0 , \\ \dot{a}_3 + \omega_1 a_2 - \omega_2 a_1 &= 0 , \\ \dot{\beta}_1 + \omega_2 \beta_3 - \omega_3 \beta_2 &= 0 , \\ \dot{\beta}_2 + \omega_3 \beta_1 - \omega_1 \beta_3 &= 0 , \\ \dot{\beta}_3 + \omega_1 \beta_2 - \omega_2 \beta_1 &= 0 , \\ \dot{\gamma}_1 + \omega_2 \gamma_3 - \omega_3 \gamma_2 &= 0 , \\ \dot{\gamma}_2 + \omega_3 \gamma_1 - \omega_1 \gamma_3 &= 0 , \\ \dot{\gamma}_3 + \omega_1 \gamma_2 - \omega_2 \gamma_1 &= 0 , \end{aligned}$$

giving a total of 12 equations that must be integrated to get the orientation of the sub-satellite as a function of time by using the method of direction cosines.

If initial conditions are given in terms of Euler angles and their first derivatives, we can use the following conversion equations:

$$\alpha_1 = \cos \psi \cos \phi - \cos \theta \sin \phi \sin \psi ,$$

$$\alpha_2 = -\sin \psi \cos \phi - \cos \theta \sin \phi \cos \psi ,$$

$$\alpha_3 = \sin \theta \sin \phi ,$$

$$\beta_1 = \cos \psi \sin \phi + \cos \theta \cos \phi \sin \psi ,$$

$$\beta_2 = -\sin \psi \sin \phi + \cos \theta \cos \phi \cos \psi ,$$

$$\beta_3 = -\sin \theta \cos \phi ,$$

$$\gamma_1 = \sin \psi \sin \theta ,$$

$$\gamma_2 = \cos \psi \sin \theta ,$$

$$\gamma_3 = \cos \theta ,$$

$$\omega_1 = \dot{\phi} \sin \theta \sin \psi + \dot{\theta} \cos \psi ,$$

$$\omega_2 = \dot{\phi} \sin \theta \cos \psi - \dot{\theta} \sin \psi ,$$

$$\omega_3 = \dot{\phi} \cos \theta + \dot{\psi} .$$

To interpret the results in terms of Euler angles, the following equations are used:

$$\tan \phi = -\frac{\alpha_3}{\beta_3} = -\frac{\sin \theta \sin \phi}{-\sin \theta \cos \phi} = \frac{\sin \phi}{\cos \phi} ,$$

$$\tan \psi = \frac{\gamma_1}{\gamma_2} = \frac{\sin \psi \sin \theta}{\cos \psi \sin \theta} = \frac{\sin \psi}{\cos \psi} ,$$

$$\tan \theta = \frac{\sqrt{\gamma_1^2 + \gamma_2^2}}{\gamma_3} = \frac{\sqrt{\sin^2 \psi \sin^2 \theta + \cos^2 \psi \sin^2 \theta}}{\cos \theta} = \frac{|\sin \theta|}{\cos \theta} .$$

There is an unavoidable ambiguity in the sign of θ , which has been chosen to be positive here for convenience.

If $\theta = 0^\circ$, the angles ϕ and ψ cannot be determined separately. However, the sum of the angles can be computed from

$$\begin{aligned} \tan(\phi + \psi) &= \frac{\beta_1}{a_1} \\ &= \frac{\cos \psi \sin \phi + \cos \theta \cos \phi \sin \psi}{\cos \psi \cos \phi - \cos \theta \sin \phi \sin \psi} \\ &= \frac{\cos \psi \sin \phi + \cos \phi \sin \psi}{\cos \psi \cos \phi - \sin \phi \sin \psi} \quad (\theta = 0) \\ &= \frac{\sin(\phi + \psi)}{\cos(\phi + \psi)} \end{aligned}$$

As a simple test case, let us use a solid ball of mass M and radius r . The moment of inertia I is

$$I = \frac{2}{5} M r^2$$

III-1.5 Test Runs of the Short Dumbbell Program with a Rigid Body at One End

As part of the process of testing the short dumbbell program, various cases have been run with different initial conditions. The program plots the tension in the wire plus the in-plane and out-of-plane motion of the point of attachment.

The simplest test run was that of a subsatellite with no initial angular velocity and no initial angular displacement; linear and angular damping were included. An in-plane displacement developed initially as the wire rotated at the orbital angular velocity. Within about 15 sec, the subsatellite acquired the orbital angular velocity and followed the angle of the wire.

Next, the subsatellite was given a 20° in-plane rotation from equilibrium with linear and angular damping. As the angle returned to equilibrium, the tension at first decreased to a minimum value in about 2 or 3 sec, increased to a maximum value at

about 9 sec, and returned to the initial value in about 20 to 25 sec. When the same case was rerun, leaving out the angular damping but keeping the linear damping, the subsatellite executed an angular oscillation of slowly decreasing amplitude. The slight damping observed results from the linear damping term, since the oscillation causes periodic changes in the length of the wire.

Next, the subsatellite was given a 20° rotation from equilibrium in a diagonal direction from the orbital plane (i. e., both in-plane and out-of-plane displacement) with both linear and angular damping. A plot of the in-plane versus out-of-plane displacement of the point of attachment shows that it returns nearly to equilibrium and then executes a small amplitude rotation about the equilibrium position with constant wire tension. The same case with no damping shows an up-and-down spring oscillation combined with a rotational oscillation in the plane of the initial rotational displacement.

In the last case run, a 20° initial diagonal rotation was combined with in-plane and out-of-plane initial angular velocities with linear and angular damping. The point of attachment ended up rotating in a small circle around the equilibrium, and the center of mass acquired a velocity diagonal to the orbital plane.

ANNEX III

ROTATIONAL DYNAMICS OF SUBSATELLITE VEHICLE

D. A. Arnold

III-2. SOFTWARE DOCUMENTATION

This program integrates the motion of two bodies connected by a massless tether. One body (the Shuttle) is assumed to be a point mass, and the second (the subsatellite) is free to rotate about the point of attachment of the wire. The program does not normally read any data cards. Instead, Fortran is compiled each time the program is run. In this way, any parameters or formulas can be changed as needed. Generally the subroutines remain unchanged. The following list describes the variables that are most likely to be changed:

TFINAL	= number of seconds for which the motion is to be integrated.
DELT	= interval at which the results are to be printed (sec).
E	= elasticity of the wire material (cgs).
DIAM	= diameter of the wire (cm).
RLO	= initial distance between the ends of the wire (cm).
RM1	= mass of the subsatellite (g).
RM2	= mass of the Shuttle (g).
RMGAL	= value of a gravity anomaly covering $1^\circ \times 1^\circ$ on the earth's surface (mgal).
XA, YA, ZA	= coordinates of the gravity anomaly on the earth's surface (cm).
HEIGHT	= height of the Shuttle above the earth (cm).
ECC	= orbital eccentricity.
B	= linear damping coefficient.
STRETCH	= initial stretch of the wire (cm).
CDRAG1	= drag coefficient of the subsatellite.
CDRAG2	= drag coefficient of the Shuttle.
AREA1	= cross-section area of the subsatellite.
AREA2	= cross-section area of the Shuttle.
RO	= atmospheric-density coefficient (g/cc).
HH	= atmospheric-density scale height (cm).
HO	= reference height for atmospheric density.
RJ2	= J_2 gravitational coefficient.

RINC	= orbital inclination (rad);
THETA, PHI, PSI	= initial Euler angles of the subsatellite (rad).
DTHETA, DPHI, DPSI	= initial time derivatives of the Euler angles.
RADIUS	= radius of the subsatellite (cm).
XI, YI, ZI	= principal moments of inertia of the subsatellite.
RB	= unit vector directed from the center of the subsatellite toward the point of attachment of the wire.

At each output point, the program prints the following variables giving information on the translational part of the motion:

TOUT	= time.
JSTART	= order of the integration polynomial.
X1, X2, } Y1, Y2, } Z1, Z2 }	= coordinates of the subsatellite and Shuttle with respect to the center of the earth.
R1, R2	= distances of the vehicles from the center of the earth.
ALONG, } ACROSS, } RADIAL }	= along-track, across-track, and radial displacements of the point of attachment of the wire with respect to the Shuttle.
RL	= separation of the Shuttle from the point of attachment of the wire.
TEN	= wire tension.
RLP	= separation rate of the vehicles.
NSTEP	= integration step number.
FRICT	= linear damping force.
H	= integration step size.

The angular information is printed by subroutine ANGOUT. The final state vector is printed and punched. The program plots the tension, along-track, and across-track displacements as a function of time using the printer page as a graph. It also plots the along-track versus the across-track displacements to give a visual display of the swinging motions of the subsatellite.

III-2.1 FUNCTION DOT (A, B)

This routine returns the quantity $\vec{A} \cdot \vec{B}$ as the value of the function.

Input Parameter

\vec{A}, \vec{B} = the vectors whose dot product is to be computed.

Output parameter

DOT = the dot product of \vec{A} and \vec{B} .

III-2.2 FUNCTION XMAG (A, U)

This routine returns the magnitude of the vector \vec{A} as the value of the function, and a unit vector parallel to \vec{A} as the vector \vec{U} .

Input Parameter

\vec{A} = any vector.

Output Parameter

\vec{U} = the vector \vec{A} divided by its magnitude.

XMAG = the magnitude of the vector \vec{A} .

III-2.3 SUBROUTINE CROSS (A, B, C)

This subroutine computes the vector \vec{C} by the equation

$$\vec{C} = \vec{A} \times \vec{B} .$$

Input Parameter

\vec{A}, \vec{B} = any vectors.

Output Parameter

\vec{C} = the cross product of the vectors \vec{A} and \vec{B} .

III-2.4 SUBROUTINE DIFROT (T, Y, DD)

This subroutine computes the derivatives of the nine direction cosines and three components of the angular velocity. The time T is not used.

Input Parameters

T = time (sec).
Y = rotational part of the state vector.

Output Parameter

DD = derivatives of the quantities in the state vector Y.

Subroutines called are CROSS, XMAG, and DOT.

III-2.5 SUBROUTINE DIFFUN (T, Y, DD)

This subroutine computes the vector DD from the state vector Y. The time T is not used. The forces included are the central gravitational force, the tension, if any, in the tether and optional perturbations due to atmospheric drag, a gravity anomaly, and J_2 .

Input Parameters

T = time (sec).
Y = positional and angular state vector

Output Parameter

DD = the derivatives of the quantities in the state vector Y.

This subroutine calls SETUP, and DIFROT.

III-2.6 SUBROUTINE SETUP (Y, IFLAG)

This subroutine does a variety of intermediate calculations necessary either for output or for calculating forces in subroutine DIFFUN. The results are placed in common.

Input Parameters

- Y** = positional and rotational state vector.
IFLAG = 1 if Y is a one-dimensional array
= 2 if Y is a two-dimensional array.

Common Variables

- RB** = the components along the body axes of the vector from the center of the subsatellite to the point of attachment of the wire.
RK = the spring constant of the wire.
RLO = the natural length of the wire.
B = the damping coefficient for the spring oscillations.
GM = the product of the gravitational constant and the mass of the earth.
RM1 = the mass of the rigid body.
RM2 = the mass of the shuttle.
RO = the atmospheric density at height HO (g/cm^3).
HO = the height at which the atmospheric density is RO.
HH = the scale height for the atmospheric density.

Output Parameters

Common Variables

- RS** = the components along the space axes of the vector from the center of the subsatellite to the point of attachment of the wire.
DX, DY, DZ = the components along the space axes of the vector from the point of attachment of the wire on the subsatellite to the Shuttle.
W = the components along the space axes of the angular momentum.
DVX, DVY, DVZ = the components along the space axes of the velocity of the Shuttle minus the velocity of the point of attachment of the wire on the subsatellite.

RL	= the distance between the ends of the wire.
TEN	= the elastic force in the wire.
RLP	= the time derivative of RL.
FRICT	= the damping force due to the rate of change of RL.
FWIRE	= the tension in the wire due to elasticity and damping.
R1SQ	= the square of the distance from the center of the earth to the center of the subsatellite.
R2SQ	= the square of the distance from the center of the earth to the Shuttle.
R1	= the square root of R1SQ.
R2	= the square root of R2SQ.
FG1	= the central gravitational force on the subsatellite divided by R1.
FG2	= the central gravitational force on the Shuttle divided by R2.
V1SQ	= the square of the velocity of the subsatellite.
V2SQ	= the square of the velocity of the Shuttle.
V1	= the velocity of the subsatellite.
V2	= the velocity of the Shuttle.
CONS1	= the atmospheric drag on the subsatellite divided by V1.
CONS2	= the atmospheric drag on the Shuttle divided by V2.

This routine calls CROSS, which computes the cross product of two vectors.

III-2.7 SUBROUTINE ANGOUT (Z, XI, YI, ZI, TOUT, JSTART, NSTEP)

This subroutine prints the angular part of the subsatellite state vector. The output information is the time, order of the integration polynomial, step number, Euler angles, a modified set of Euler angles consisting of successive rotations about the x, y, and z axes, the components of angular momentum along the space axes, the components of angular momentum about the body axes, the components of angular velocity about the space axes, and the components of angular velocity about the body axis.

Input Parameters

Z	= the nine direction cosines giving the orientation of the body axes with respect to the inertial axes, plus the three components of the angular velocity with respect to the body axes.
XI, YI, ZI	= the principle moments of inertia.
TOUT	= time.
JSTART	= the order of the polynomial used on the current integration step.
NSTEP	= the step number.

No other subroutines are called by this routine.

III-2.8 SUBROUTINE ROTSTAT (THETA, PHI, PSI, DTHETA, DPHI, DPSI, Y, A)

This subroutine computes the nine direction cosines and three angular velocities from the Euler angles and their derivatives. Also computed are the components of the vector from the center of mass of the satellite to the point of attachment of the wire in the inertial coordinate system.

Input Parameters

THETA	=	θ .
PHI	=	ϕ .
PSI	=	ψ .
DTHETA	=	$\dot{\theta}$.
DPHI	=	$\dot{\phi}$.
DPSI	=	$\dot{\psi}$.

θ , ϕ , and ψ are the Euler angles defining the orientation of the body axes with respect to the inertial axes. $\dot{\theta}$, $\dot{\phi}$, and $\dot{\psi}$ are the time derivatives of the Euler angles.

Common Variables

RADIUS	=	the distance from the center of mass of the rigid body to the point of attachment of the wire.
RB	=	a unit vector pointing from the center of mass of the subsatellite to the point of attachment of the wire. The components are taken along the body axes.

Output Parameters

A	=	nine direction cosines relating the body axes to the inertial axes, plus the three components of the angular velocity on the body axes.
Y	=	a matrix containing the translational state vector plus the rotational state vector A.

Common Variable

RS	=	the vector from the center of mass of the subsatellite to the point of attachment of the wire. The components are along the inertial axes.
----	---	--

No other subroutines are called by this routine.